European Journal of Medicinal Chemistry 61 (2013) 26–40

Contents lists available at SciVerse ScienceDirect

European Journal of Medicinal Chemistry

journal homepage: http://www.elsevier.com/locate/ejmech

Original article

Structure-based optimization of oxadiazole-based GSK-3 inhibitors

Fabio Lo Monte [a,*], Thomas Kramer [a], Jiamin Gu [a], Martin Brodrecht [a], Johannes Pilakowski [a], Ana Fuertes [b], Juan Manuel Dominguez [b], Batya Plotkin [c], Hagit Eldar-Finkelman [c], Boris Schmidt [a,*]

[a] Clemens Schöpf – Institute of Organic Chemistry and Biochemistry, Technische Universität Darmstadt, Petersenstrasse 22, 64287 Darmstadt, Germany
[b] Noscira S.A., Drug Discovery, Tres Cantos 28760 Madrid, Spain
[c] Department of Human Molecular Genetics and Biochemistry, Sackler School of Medicine, Tel Aviv University, 69978 Tel Aviv, Israel

ARTICLE INFO

Article history:
Received 16 March 2012
Received in revised form
16 May 2012
Accepted 3 June 2012
Available online 12 June 2012

Keywords:
Glycogen synthase Kinase-3 (GSK-3)
Alzheimer's disease
Structure–activity relationship (SAR)
Reversible inhibition
Zebrafish phenotype

ABSTRACT

Inhibition of glycogen synthase kinase-3 (GSK-3) induces neuroprotective effects, e.g. decreases β-amyloid production and reduces tau hyperphosphorylation, which are both associated with Alzheimer's disease (AD). The two isoforms of GSK-3 in mammalians are GSK-3α and β, which share 98% homology in their catalytic domains. We investigated GSK-3 inhibitors based on 2 different scaffolds in order to elucidate the demands of the ATP-binding pocket [1]. Particularly, the oxadiazole scaffold provided potent and selective GSK-3 inhibitors. For example, the most potent inhibitor of the present series, the acetamide **26d**, is characterized by an IC_{50} of 2 nM for GSK-3α and 17 nM for GSK-3β. In addition, the benzodioxane **8g** showed up to 27-fold selectivity for GSK-3α over GSK-3β, with an IC_{50} of 35 nM for GSK-3α. Two GSK-3 inhibitors were further profiled for efficacy and toxicity in the wild-type (wt) zebrafish embryo assay to evaluate simultaneously permeability and safety.

1. Introduction

Alzheimer's disease (AD) is a neurodegenerative disorder and characterized by the presence of abnormal filamentous protein inclusions in nerve cells of the brain [2]. The neuropathological hallmarks of AD were first reported by Alois Alzheimer and date back to 1907 [3,4]. These inclusions are formed by extracellular amyloid deposits and intracellular microtubule-associated protein tau [5]. Early onset forms of familial Alzheimer's disease (FAD) have been linked to mutations in the amyloid precursor protein (APP), presenilin-1 (PS-1) and presenilin-2 (PS-2). These mutations adversely affect APP processing and result in the increased production of the 40-42 amino acid long β-amyloid (Aβ) peptides, which are the major component of amyloid deposits. Several risk factors have been associated with sporadic Alzheimer's disease (SAD). The most prevalent is aging and the presence of specific ApoE isoforms, which have been implicated in Aβ clearance. The activation of β-secretase may be involved in Aβ generation, which in combination with a deficiency in Aβ clearance will result in the accumulation of Aβ aggregates [2,6]. Partially phosphorylated tau in the normal adult brain features sequences that support association with tubulin, which entails the stabilization of microtubules. The pathological hyperphosphorylation of tau causes destabilization of microtubules, which in turn interferes with tubulin binding. The misfolding of hyperphosphorylated tau leads to the formation of insoluble neurofibrillary tangles (NFTs) and intraneuronal aggregates of paired helical filaments (PHFs) [7,8]. GSK-3 was shown to phosphorylate tau both *in vitro* and *in vivo* on multiple sites [7]. Several studies demonstrate that inhibition of GSK-3 induces decreased Aβ production and a reduction in tau hyperphosphorylation [9,10]. GSK-3 was identified in the late 1970s and is a constitutively active, ubiquitously expressed serine/threonine kinase, which participates in a number of physiological processes [2,11]. Two related isoforms of GSK-3 exist in mammals, GSK-3α and β, which share 98% homology in their catalytic domains and have similar biochemical properties [7,12]. The isoforms differ significantly outside of their catalytic domains at their N-terminal regions [13]. Furthermore, an alternative splice variant of GSK-3β: GSK-3β2, has been reported for rodents and humans [14,15]. The crystal structure of GSK-3β was determined in 2001 [16,17]. GSK-3 is highly enriched in the brain and several publications indicate that the GSK-3β isoform is a key kinase required for abnormal hyperphosphorylation of tau [18–20]. Lithium chloride was the first GSK-3 inhibitor to be discovered. However there are several other biological targets for lithium cations, which impose limits on the therapeutic window. Considering the homology of GSK-3α and β within the ATP-binding pocket it appears difficult to identify an

* Corresponding authors. Tel.: +49 6151 164531; fax: +49 6151 163278.
E-mail addresses: Fabio.Lo-Monte@gmx.de (F. Lo Monte), schmidt_boris@t-online.de (B. Schmidt).

0223-5234/$ – see front matter © 2012 Elsevier Masson SAS. All rights reserved.
http://dx.doi.org/10.1016/j.ejmech.2012.06.006

inhibitor that differentiates the two isoforms. All GSK-3 inhibitors developed until now are able to inhibit the two isoforms with almost similar potency, except compound **Λ-OS1**, which showed up to 7-fold selectivity for GSK-3α and compound **15b**, which showed up to 92-fold selectivity for GSK-3α [21–24]. A plethora of GSK-3 inhibitors has been described and most of the effects were observed *in vitro* and cellular studies (Fig. 1) [5,25,26]. These studies and the ongoing patent filing indicate that GSK-3 is a potential drug target not just for the treatment of AD. Several research groups and pharmaceutical companies are interested in the discovery of novel GSK-3 inhibitors with good selectivity and bioavailability despite of the Wnt-pathway associated risks, which may result in adverse cell proliferation. In the present study, the 1,3,4-oxadiazole-moiety served as a scaffold for a variety of GSK-3 inhibitors. This particular heterocycle was chosen because it has favorable properties over 1,2,4-oxadiazoles and other five-membered heterocycles [27]. The inhibition potencies of these compounds were compared to those of the previously reported 1,3,4-oxadiazoles and substituted ureas in the attempt to identify additional heterocycles and substituents that enhance GSK-3 inhibition [1,28–30]. The resulting interactions with the ATP-binding pocket of GSK-3α and β were also investigated to generate a hypothesis for isoform discrimination. We employed the wild-type zebrafish embryo in order to validate the utility of these compounds *in vivo*.

2. Chemistry

The esterfication of the carboxylic acids **1a**, **b** afforded compounds **2a**, **b** which were converted to the hydrazides **3a**, **b**. The hydrazide **3c** was commercially available. Reaction of the hydrazides **3a**–**c** with carbon disulfide (CS_2) afforded the oxadiazoles **4a**–**c** (Scheme 1) [28,31,32].

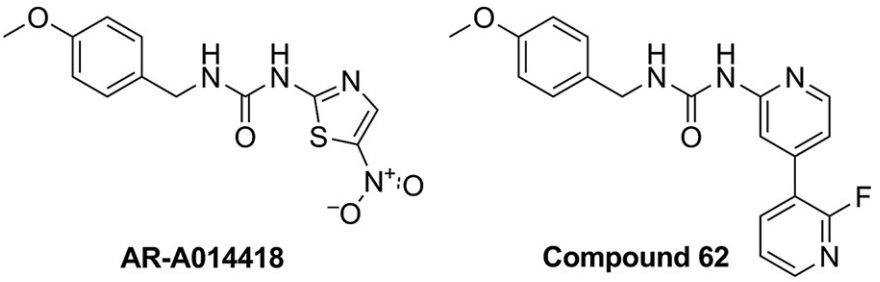

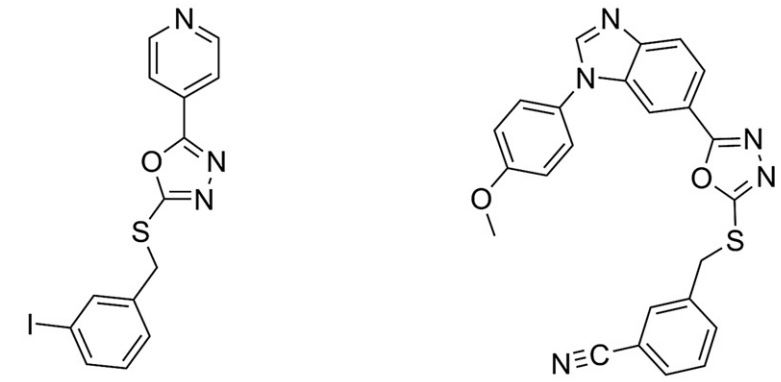

Fig. 1. Structures of previously reported GSK-3 inhibitors.

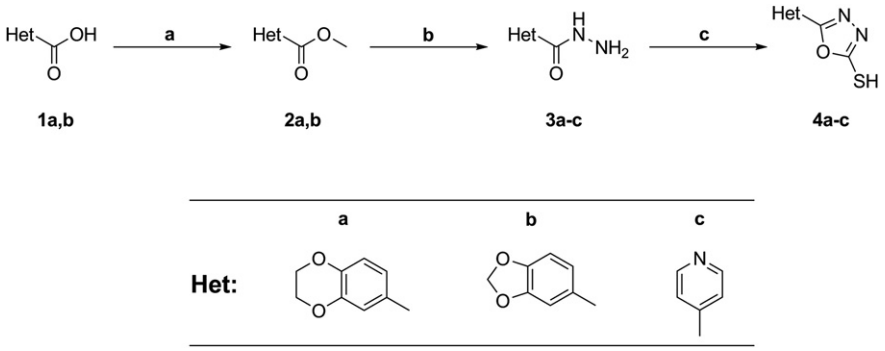

Scheme 1. Reagents and conditions: (a) MeOH, $SOCl_2$, 0 °C–50 °C, 83–89%; (b) $NH_2NH_2{\bullet}H_2O$, EtOH, reflux, 67–75%; (c) CS_2, Et_3N, EtOH, reflux, 79–89%.

The biphenyls **7a**–**h** were prepared in two steps from commercial *p*-tolylboronic acid and bromobenzene bearing substituents at the 1- to 4-position [33]. The biphenyl halides **7a**–**h** were coupled with the heterocycles **4a**–**c** to obtain the compounds **8a**–**h**, **9a**–**f** and **10a**–**f** (Scheme 2). The thioethers **15**–**18** (**a**–**d**) (Scheme 3) were synthesized similar to method described in Schemes 1 and 2 [28,34,35]. The hydrazones **20a**–**d** were prepared using isoniazid **19** (Scheme 4) and 4 different benzaldehydes [36–38]. The esterification of acid **21** to the ester **22** employed standard conditions, it was followed by reaction with acetic anhydride to provide the amide **23** (Scheme 5) [39,40]. The thioethers **26a**–**d** were synthesized according to the method described in Schemes 1 and 2. Esterfication of compound **27**, followed by cyclization gave compound **29** (Scheme 6) [41,42].

Compound **30** was obtained using the conditions described for compound **23** [40]. Saponification of the ester **30**, followed by reaction with *tert*-butyl carbazate, gave compound **32** [28,43]. Cleavage of the *tert*-butylamine in **32** by TFA and submission to the reaction conditions described in Schemes 1 and 2 provided the final product **35** [28]. Bromination of the 4-hydroxybenzoic acid **36**, gave compound **37** (Scheme 7) [44]. The dibenzofuran **38** was obtained by the combination of two reactions in a one-pot synthesis [45,46]. The final compound **41** was prepared in relation to the method described in Schemes 1 and 2. The structures of all compounds were verified by mass spectrometry, ^{1}H NMR and ^{13}C NMR.

3. Results and discussion

The synthesized compounds were evaluated for GSK-3 inhibition in a commercial system based on the Z′-LYTE® technology, available from Invitrogen Life Technologies (Carlsbad, CA, USA), using human recombinant GSK-3α or GSK-3β as the enzyme source and further for their inhibitory activity *in vitro* against GSK-3β. Several compounds displayed more than 50% inhibitory activity against GSK-3β at 10 μM concentration. We focussed our interest on inhibitors with potential occupation of the entire ATP-binding pocket, and thereby to enhance potency and selectivity (Fig. 2). Heterocycles featuring the oxadiazole ring typically interact within the green marked area of GSK3 (Fig. 2). Our goal was to extend our compounds to the area highlighted in blue. Furthermore, we tried to enhance the potential interaction with the backbone by replacing heterocycles with phenyl rings bearing different acceptors and to investigate the contribution deriving from the rigidity of a tricyclic system [26]. The 3 heterocyclic fragments **4a**–**c** were introduced as potential hinge binders in order to interact with the GSK-3 backbone: Asp133/Tyr134/Val135 (Scheme 1). The oxadiazole moiety is assumed to engage with the polar binding pocket, consisting of three amino acids (Lys85/Glu97/Asp200). Such interactions were previously reported for the GSK-3β inhibitor II and 20x (Fig. 1). We coupled the compounds **4a**–**c** to biphenyl systems bearing different substituents on the second phenyl ring (Scheme 2). Most of these compounds showed remarkable activities and selectivities (Table 1).

The compounds **8f** and **9a**–**e** were found to be potent inhibitors of both isoforms of GSK-3 as characterized by IC_{50} values in the low nanomolar range. In addition, all of them showed good selectivities against other kinases. Substituents in the ortho- and para-positions of structure **8** and **9** lead to potent inhibition of both isoforms as indicated for compound **8f** and **9e** with an IC_{50} value of 5 nM for GSK-3α respectively 14 nM and 32 nM for GSK-3β. We reasoned

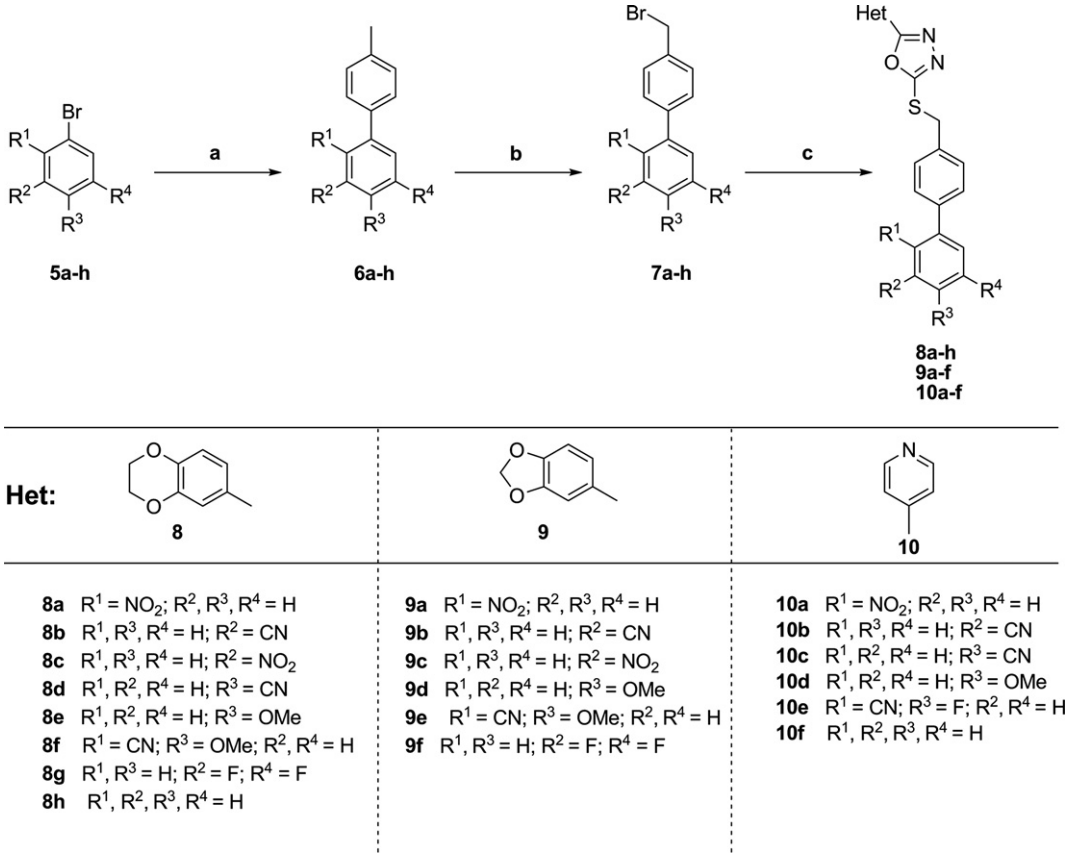

Scheme 2. Reagents and conditions: (a) aryl bomide, toluene, EtOH, $Pd(PPh_3)_4$, 2-tolylboronic acid, 2 N Na_2CO_3(aq.), 80 °C; (b) NBS, AIBN, CCl_4, reflux; (c) oxadiazoles (4a-c), 1 N NaOH, DMF, rt, 27–79%.

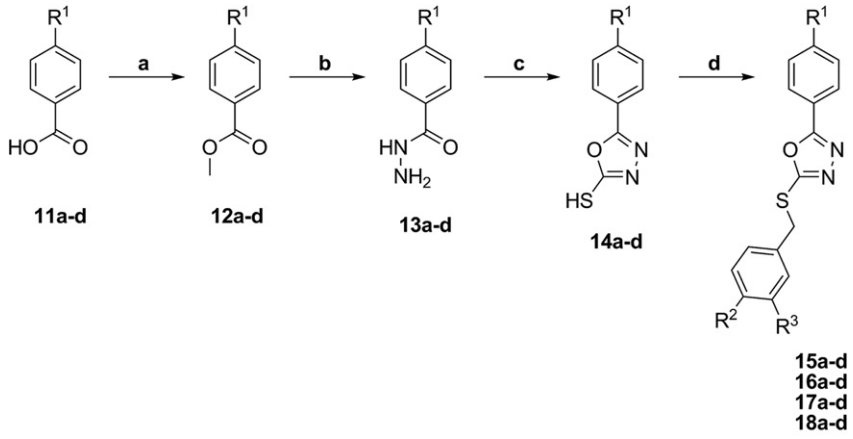

15a R^1, R^2, R^3 = H
15b R^1 = H, R^2 = 2-benzonitrile; R^3 = H
15c R^1 = H; R^2 = H, R^3 = OMe
15d R^1 = H; R^2 = H, R^3 = CN

16a R^1 = OMe; R^2, R^3 = H
16b R^1 = OMe, R^2 = 2-benzonitrile; R^3 = H
16c R^1 = OMe; R^2 = H, R^3 = OMe
16d R^1 = OMe; R^2 = H, R^3 = CN

17a R^1 = CN; R^2 = H, R^3 = H
17b R^1 = CN, R^2 = 2-benzonitrile; R^3 = H
17c R^1 = CN; R^2 = H, R^3 = OMe
17d R^1 = CN; R^2 = H, R^3 = CN

18a R^1 = NO_2; R^2 = H, R^3 = H
18b R^1 = NO_2, R^2 = 2-benzonitrile; R^3 = H
18c R^1 = NO_2; R^2 = H, R^3 = OMe
18d R^1 = NO_2; R^2 = H, R^3 = CN

Scheme 3. Reagents and conditions: Reagents and conditions: (a) MeOH, $SOCl_2$, 0 °C–50 °C, 68–76%; (b) $NH_2NH_2{\bullet}H_2O$, EtOH, reflux, 81–89%; (c) CS_2, Et_3N, EtOH, reflux, 74–88%; (d) Benzyl halides, 1 N NaOH, DMF, rt, 32–71%.

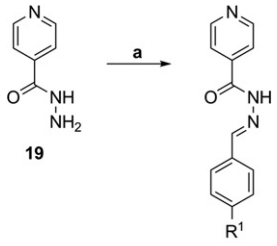

20a R^1= H
20b R^1 = OMe
20c R^1 = CN
20d R^1 = ethyl

Scheme 4. Reagents and conditions: (a) EtOH/H_2O, Aldehydes, rt, 83–97%.

that only the interplay respectively combination of different substituents is adequate to gain selectivity against one GSK-3 isoform. Compounds **8b** and **8g** enhance the selectivity for GSK-3α up to 27-fold. An inverse effect was observed for pyridine **10e** where a substituent in meta- and para-position leads to slightly increased selectivity for inhibition of GSK-3β. All compounds lacking the heterocycle (Scheme 3) or oxadiazole ring (Scheme 4) completely lost most of their ability to inhibit GSK-3 and resulted in a residual GSK-3β activity of more than 50% at 10 μM. We attempted the combination of different lead structures by the addition of an amide function at the pyridine and benzothiazole (Schemes 4 and 5). A similar moiety serves as an ambident moiety on Sorafenib. It was reported to establish hydrogen bonds with the same amide on the target hinge region either via the pyridyl nitrogen or through the carbonyl of the acetyl amide [47,48].

Thus the amide was expected to increase the interaction with the backbone of GSK-3 as observed in the tight binding of Compound **62** and **AR-A014418** (Fig. 1). We determined promising activities and selectivities for the pyridines **26a**, **26c** and **26d**. Especially compound **26d** with an IC_{50} value of 2 nM for GSK-3α and 17 nM for GSK-3β showed more than 5000-fold selectivity against Cdk5/p35, CK1ε, AurKA and PKCα (Table 1). However, the additional amide on the benzothiazole **35** reduced activity for both isoforms indicating too close proximity to the backbone. Moreover, the acetamide **26d** is characterized by a clogP of 2.90 and a tPSA of 103.0 $Å^2$. The letter value exceeds the limits for likely blood–brain

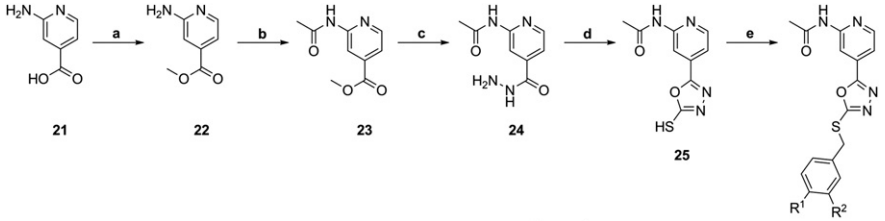

26a R^1 = H; R^2 = H
26b R^1 = H; R^2 = OMe
26c R^1 = H; R^2 = CN
26d R^1 = 2-benzonitrile; R^2 = H

Scheme 5. Reagents and conditions: (a) MeOH, $SOCl_2$, 0 °C–50 °C, 89%; (b) acetic anhydride, 105 °C, 69%; (c) $NH_2NH_2{\bullet}H_2O$, EtOH, reflux, 74%; (d) CS_2, Et_3N, EtOH, reflux, 92%; (e) Benzyl halides, 1 N NaOH, DMF, rt, 37–68%.

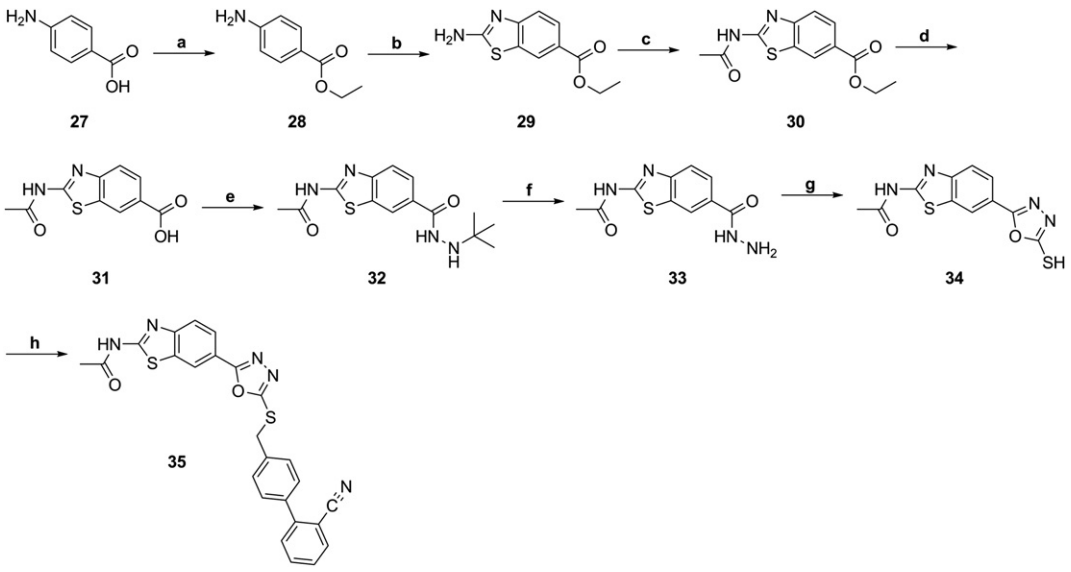

Scheme 6. Reagents and conditions: (a) EtOH, H_2SO_4, reflux, 91%; (b) CH_3COOH, KSCN, Br_2, rt, 67%; (c) acetic anhydride, 105 °C, 58%; (d) MeOH, 1 N NaOH, rt, 94%; (e) DMF, *tert*-Butyl carbazate, EDCI, HOBt•H_2O, rt, 77%; (f) TFA, rt, 99%; (g) CS_2, Et_3N, EtOH, reflux, 81%; (h) Benzyl halide, 1 N NaOH, DMF, rt, 47%.

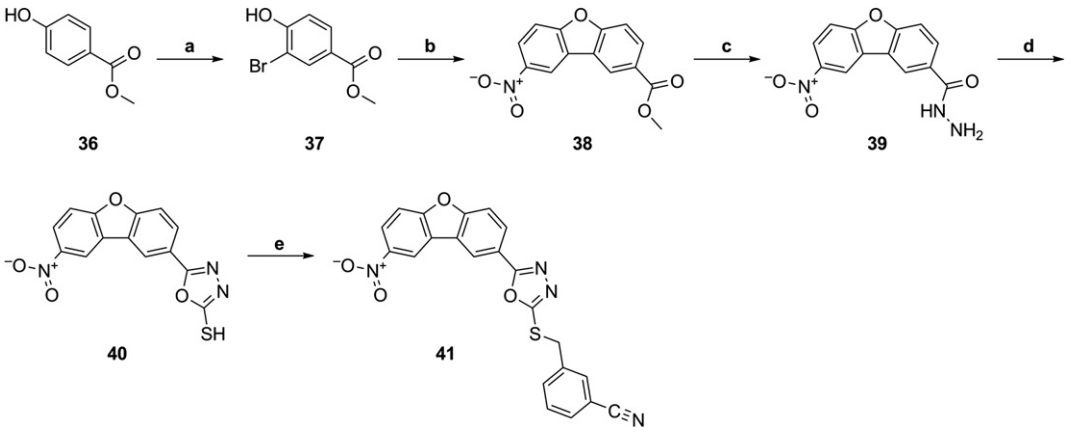

Scheme 7. Reagents and conditions: (a) DCM, Br_2, rt, 65%; (b) DMF, $Pd(OAc)_2$, K_2CO_3, 130 °C, 30%; (c) NH_2NH_2•H_2O, rt, 99%; (d) CS_2, Et_3N, EtOH, reflux, 48%; (e) Benzyl halide, 1N NaOH, DMF, rt, 44%.

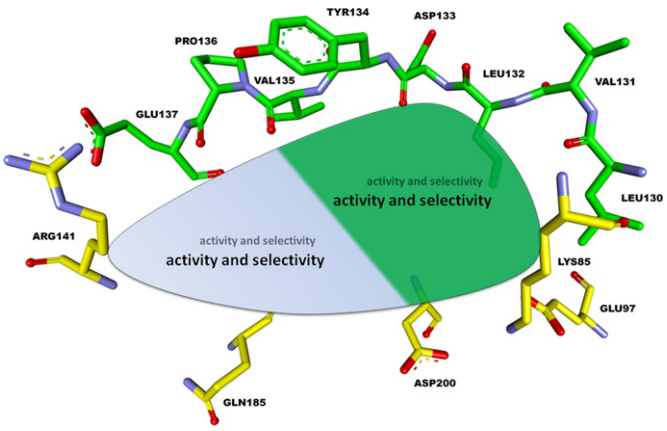

Fig. 2. Schematic overview of the GSK-3 ATP-binding pocket. The green marked area reveals the interaction site of the heterocycle and oxadiazole ring. The area we wanted to occupy with our structures is marked light blue. (For interpretation of the references to colour in this figure legend, the reader is referred to the web version of this article.)

barrier permeation. In addition, the structural rigidity of the dibenzofuran **41** resulted in loss of inhibitory activity against GSK-3.

A docking study of compound **9e** and **26d** into the PDB structure 3F88 of GSK-3β suggested a binding mode that uses the ATP-binding pocket in its entirety. The oxadiazole interacts in both cases with the polar pocket consisting of Lys85 and Asp200. For compound **9e** the amide functions leads to a binding mode along the hinge region of the ATP-binding pocket. The biphenyl system interacts with Ile62, Gly63, Phe67 and Val70, which form part of the flexible glycine-rich loop. The methoxy group of compound **9e** is located in close proximity to the salt bridge formed by Glu137 and Arg141, which may be responsible for the activity of this compound. Nevertheless, this structure does not provide insight into the selective inhibition of the GSK-3β isoforms as all amino acid residues shown in Fig. 3 are identical in both isoforms. Hence, only a complex of GSK-3β co-crystallized with one of these inhibitors, solved by X-ray crystallography, may provide the necessary insights. After evaluation of the *in vitro* activity and selectivity of these compounds the biphenyl derivatives **9e** and **26d** were.further tested for their *in vivo* activity on wt zebrafish embryos. We

Table 1
Inhibitory activity against different kinases *in vitro* and *in silico* parameters (calc. with ChemDraw Ultra 9.0.1).

IC_{50} (μM)							clogP	tPSA(Å^2)
Compound	GSK-3α	GSK-3β	Cdk5/p35	CK1ε	AurKA	PKCα		
8a	0.004	0.090	>100	>100	>100	>100	4.62	112.2
8b	0.009	0.225	>100	>100	>100	>100	4.31	84.8
8c	0.015	0.164	>100	>100	>100	>100	4.62	112.2
8d	0.195	1.995	>100	>100	50.0	>100	4.31	84.8
8e	0.019	0.127	>100	>100	>100	>100	4.80	79.0
8f	0.005	0.032	>100	>100	>100	>100	4.56	98.9
8g	0.035	0.966	>100	>100	>100	>100	5.16	64.9
8h	0.051	0.234	>100	>100	>100	>100	4.88	64.9
9a	0.003	0.027	>100	>100	>100	>100	4.66	112.2
9b	0.004	0.029	>100	>100	>100	>100	4.35	84.8
9c	0.015	0.086	>100	>100	>100	>100	4.66	112.2
9d	0.007	0.075	>100	20.0	40.0	>100	4.84	79.0
9e	0.005	0.014	>100	50.0	45.0	>100	4.60	98.9
9f	0.051	0.195	>100	80.0	>100	>100	5.21	64.9
10a	0.027	0.164	>100	>100	5.0	>100	3.28	95.3
10b	0.046	0.084	>100	>100	60.0	>100	2.97	67.9
10c	0.077	0.153	>100	>100	>100	>100	2.97	67.9
10d	0.240	0.176	>100	>100	>100	>100	3.45	62.1
10e	0.324	0.056	>100	>100	>100	>100	3.11	67.9
10f	0.052	0.083	>100	>100	>100	>100	3.53	48.0
26a	0.020	0.035	>100	>100	60.0	>100	1.58	83.1
26c	0.017	0.019	>100	>100	>100	>100	1.01	103.0
26d	0.002	0.017	>100	>100	>100	>100	2.90	103.0

exposed the embryos to these compounds at early stages of development (Fig. 4). The embryos were collected and maintained in E2 medium at ~28 °C. The compounds were added 5 hpf (hour post fertilization), and the phenotypes were compared at 44-48 hpf. Compounds **9e** and **26d** cause a stunted and crooked tail at 30 μM. This correlates with the observation that Wnt signaling, and thus GSK-3β activity, plays a crucial role in the development of metazoan. This was demonstrated for the known GSK-3 inhibitors LiCl and the ruthenium complex (**R**)-**7**, which both perturb zebrafish development [49,50]. However, it must be noted that compound **9e** and **26d** were not completely dissolved in the E2-medium at 30 μM. Thus, an exact concentration cannot be stated for these compounds. Nevertheless, both compounds exerted no toxicity in the observation range (<30 μM).

4. Conclusion

In this report, we describe the synthesis and evaluation of oxadiazole-based GSK3 inhibitors. Occupation of the ATP-binding pocket in its entirety led to the identification of several potent and selective compounds. These compounds are characterized by IC_{50} values in the low nanomolar range and good selectivity versus other kinases. Surprisingly, we ascertained that the addition of different functional groups onto the biphenyl system was adequate to gain selectivity against one GSK-3 isoform. To the best of our knowledge the selectivity of compound **8g** for GSK-3α compared to GSK-3β is among the highest ever reported. These observations will be helpful, if the discrimination of one GSK-3 isoform is needed *in vivo*. The discriminating factor for this isoform selectivity is still unknown as the ATP-binding sites are almost identical in the two isoforms (Fig. 3). Differences in the amino acid sequence of the channels leading to the binding sites may hold a cue, but the lack of a crystallized GSK-3α makes this hypothesis highly speculative. Furthermore, amino acids in the second-sphere close to the ATP-binding pocket do vary for GSK-3α and thus may contribute to conformational changes. The interaction with the glycine-rich loop might have significant effects on the binding potencies and

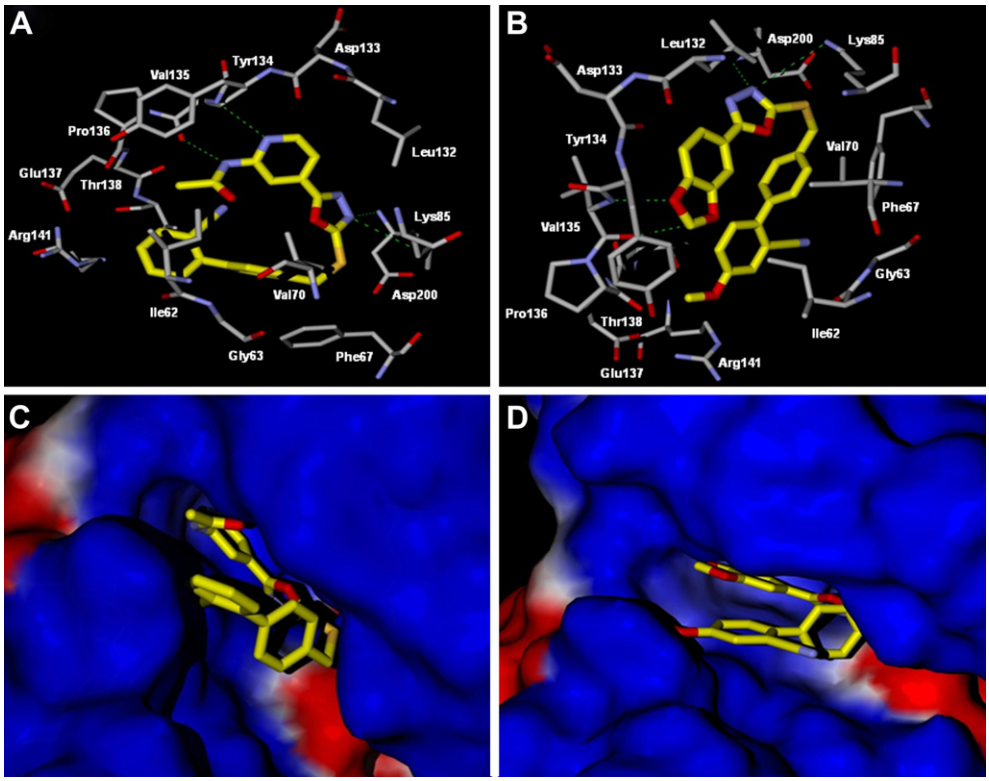

Fig. 3. Docking of compounds **9e** and **26d** into PDB structure 3F88 of GSK-3β; hydrogen bond interactions of compound **26d** (A) and **9e** (B) with the amino acids of the ATP-binding pocket; Surface illustration of the ATP-binding pocket with compound **26d** (C) and **9e** (D). The inhibitors are shown in yellow. These figures were prepared with Molegro Virtual Docker 5. (For interpretation of the references to colour in this figure legend, the reader is referred to the web version of this article.)

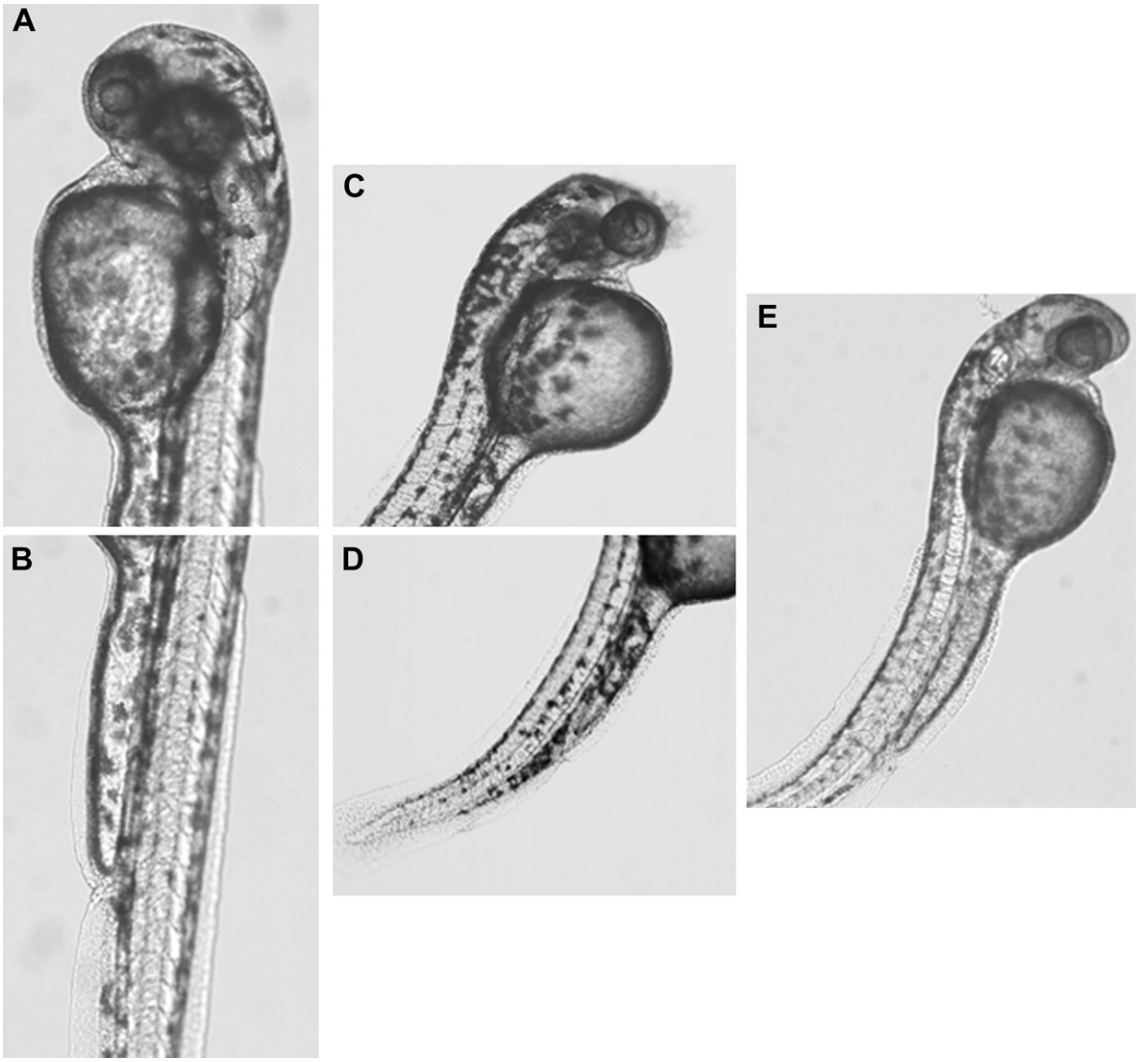

Fig. 4. Effect on the wild-type zebrafish embryo by compounds **9e** and **26d**. the embryos were collected and maintained in E2 medium at ~28 °C, compound was added 5 hpf, and the phenotypes were compared at 44–48 hpf. (A, B) Head and tail of control embryos - DMSO (2%). (C, D) Embryo treated with compound **9e**. this compound causes a stunted and crooked tail at 30 μM. (E) Embryo treated with compound **26d**. this compound causes a stunted and crooked tail at 30 μM.

selectivities of the biphenyl derivatives similar to the compounds reported by Li Feng *et al* [22]. The amide function in compound **26d** indicated a potential interaction with the backbone exploitable for further improvement. However, this moiety causes a significant contribution to the tPSA (103.0 $Å^2$) and thus impairs potential blood–brain barrier permeation. We exposed wt zebrafish embryos to two of these compounds at early stages of development and obtained desirable *in vivo* efficacy for compound **9e** and **26d**. We suppose that GSK-3α inhibition offers a new approach to reduce the formation of both amyloid plaques and neurofibrillary tangles and thus may be valuable in the treatment of AD [51]. On the basis of these results the derivatives **8b**, **8g** and **26d** were selected for further pharmacological and structural evaluations.

5. Experimental

5.1. Chemistry

All reactions under anhydrous conditions were carried out under argon atmosphere with dry solvents, unless otherwise noted. All the commercial chemicals were used without further purification. The ^1H NMR spectra were recorded on a Bruker AC 300 spectrometer at 300 MHz and Bruker AC 500 spectrometer at 500 MHz. The ^{13}C NMR spectra were recorded on a Bruker AC 300 spectrometer at 75 MHz and Bruker AC 500 spectrometer at 125 MHz. Chemical shifts are reported as ppm downfield from Me_4Si. Abbreviations used to explain the multiplicities: s = singlet, d = doublet, *t* = triplet, *q* = quartet, m = multiplet, br = broad. Coupling constants (*J* values) are given in hertz (Hz). Mass spectrometry was performed on a Bruker-Franzen Esquire LC mass spectrometer and a MAT 95 double focusing sector field MS. High performance liquid chromatographies were carried out on an Agilent 1100 (column: reversed phase, Zorbax Eclipse XDB-C8, 4.6 × 150 mm; 254 nm). Flash column chromatography was carried out using Merck silica gel 60 (40–63 and 15–40 μm) and 60G (5–40 μm). Thin-layer chromatography (TLC) was carried out using aluminum sheets precoated with silica gel 60 F254 (0.2 mm; E. Merck).

5.2. Methyl 2,3-dihydrobenzo[b][1,4]dioxine-6-carboxylate (**2a**)

To a stirred solution of 2,3-dihydrobenzo[*b*][1,4]dioxine-6-carboxylic acid **1a** (1.80 g, 10 mmol) in MeOH (20 mL) was added $SOCl_2$ (1.45 mL, 20 mmol) dropwise at 0 °C over 1 h. The mixture

was further stirred 12 h at 50 °C. The solution was cooled to room temperature and diluted with water (25 mL). MeOH was evaporated and the pH adjusted to ~6 with aqueous $NaHCO_3$. The mixture was extracted three times with EtOAc and successively washed with brine. The organic layer was dried over $MgSO_4$ and concentrated under reduced pressure to give **2a** (1.6 g, 83%) as a colorless solid. ^{1}H NMR (DMSO-d_6, 500 MHz): δ [ppm] = 3.80 (3H, s), 4.19 (2H, m), 4.23 (2H, m), 6.80 (1H, m), 7.47 (2H, m). ^{13}C NMR (DMSO-d_6, 125 MHz): δ [ppm] = 50.5, 62.7, 63.2, 115.7, 117.6, 122.0, 141.7, 146.4, 165.2. EI-MS: m/z 194 (M^+).

*5.2.1. Compound **2b** was prepared in a similar manner to that described for **2a***

Methyl benzo[*d*][1,3]dioxole-5-carboxylate (**2b**). Yield 89%, colorless solid. ^{1}H NMR (DMSO-d_6, 500 MHz): δ [ppm] = 3.81 (3H, s), 6.14 (2H, s), 7.03 (1H, d, J = 8.1 Hz), 7.38 (1H, d, J = 1.6 Hz), 7.57 (1H, dd, J = 8.1 Hz, J = 1.7 Hz). ^{13}C NMR (DMSO-d_6, 125 MHz): δ [ppm] = 52.0, 102.1, 108.2, 108.5, 123.4, 125.0, 147.6, 151.4, 165.6. EI-MS: m/z = 180 (M^+).

*5.3. 2,3-Dihydrobenzo[b][1,4]dioxine-6-carbohydrazide (**3a**)*

To a solution of **2a** (1.16 g, 6.0 mmol) in EtOH (30 mL) was added hydrazine hydrate (2.91 mL, 60 mmol) and the mixture was heated at reflux for 2 days. After cooling to room temperature pure crystals are formed, collected by filtration and washed several times with EtOH to give compound **3a** (0.87 g, 75%) as a light yellow solid. ^{1}H NMR (DMSO-d_6, 500 MHz): δ [ppm] = 4.28 (2H, m), 4.30 (2H, m), 6.89 (1H, d, J = 8.4 Hz), 7.30 (1H, dd, J = 8.3 Hz, J = 2.1 Hz), 7.33 (1H, d, J = 2.1 Hz). ^{13}C NMR (DMSO-d_6, 125 MHz): δ [ppm] = 65.9, 66.3, 117.9, 118.6, 121.9, 127.5, 145.2, 148.6, 169.6. EI–MS: m/z 194 (M^+).

*5.3.1. Compound **3b** was prepared in a similar manner to that described for **3a***

Benzo[*d*][1,3]dioxole-5-carbohydrazide (**3b**). Yield 67%, colorless solid. ^{1}H NMR (DMSO-d_6, 500 MHz): δ [ppm] = 4.42 (2H, s), 6.07 (2H, s), 6.96 (1H, d, J = 8.1 Hz), 7.35 (1H, d, J = 1.7 Hz), 7.42 (1H, dd, J = 8.1 Hz, J = 1.7 Hz), 9.59 (1H, s). ^{13}C NMR (DMSO-d_6, 125 MHz): δ [ppm] = 101.5, 106.9, 107.8, 121.8, 127.2, 147.2, 149.5, 165.2. EI-MS: m/z = 180 (M^+).

*5.4. 5-(2,3-Dihydrobenzo[b][1,4]dioxin-6-yl)-1,3,4-oxadiazole-2-thiol (**4a**)*

To a solution of **3a** (582 mg, 3.00 mmol) in EtOH (5 mL) were added carbon disulfide (397 μL, 6.60 mmol) and Et_3N (469 μL, 3.30 mmol) and the mixture was heated at reflux overnight. The reaction mixture was diluted with EtOAc and the organic layer was washed with 0.1 N HCl, brine and dried over Na_2SO_4. The solvent was evaporated under reduced pressure, and the obtained residue was recrystallized from CH/EtOAc (1:2) to give **4a** (630 mg, 89%) as a light brown solid. ^{1}H NMR (DMSO-d_6, 500 MHz): δ [ppm] = 4.32 (2H, m), 4.34 (2H, m), 7.05 (1H, d, J = 8.4 Hz), 7.30 (1H, d, J = 2.0 Hz), 7.36 (1H, dd, J = 8.4 Hz, J = 2.0 Hz), 14.2 (1H, s, br). ^{13}C NMR (DMSO-d_6, 125 MHz): δ [ppm] = 64.4, 64.8, 115.0, 115.7, 118.6, 120.0, 144.2, 147.3, 160.6, 177.6. EI-MS: m/z = 236 (M^+).

*5.4.1. Compound **4b** was prepared in a similar manner to that described for **4a***

5-(Benzo[*d*][1,3]dioxol-5-yl)-1,3,4-oxadiazole-2-thiol (**4b**). Yield 79%, pale yellow solid. ^{1}H NMR (DMSO-d_6, 500 MHz): δ [ppm] = 6.14 (2H, s), 7.10 (1H, d, J = 8.1 Hz), 7.33 (1H, d, J = 1.6 Hz), 7.42 (1H, dd, J = 8.1 Hz, J = 1.6 Hz). ^{13}C NMR (DMSO-d_6, 125 MHz): δ [ppm] = 102.1, 105.6, 109.1, 116.1, 121.5, 148.1, 150.6, 160.3, 177.2. EI-MS: m/z = 222 (M^+).

*5.4.2. Compound **4c** was prepared in a similar manner to that described for **4a***

5-(Pyridin-4-yl)-1,3,4-oxadiazole-2-thiol (**4c**). Yield 83%, yellow solid. ^{1}H NMR (DMSO-d_6, 500 MHz): δ [ppm] = 7.81 (2H, dd, J = 4.4 Hz, J = 1.6 Hz), 8.81 (2H, dd, J = 4.4 Hz, J = 1.6 Hz). ^{13}C NMR (DMSO-d_6, 125 MHz): δ [ppm] = 119.6, 129.7, 150.8, 158.7, 177.8. EI-MS: m/z = 179 (M^+).

*5.5. General procedure for synthesis of compounds **6a–h** [33]*

To a solution of the aryl bromide (5 mmol) in 15 mL of toluene/EtOH (1/1) was added 0.17 g (0.14 mmol) of $Pd(PPh_3)_4$, and the mixture was stirred under argon atmosphere. Then 2 N aqueous Na_2CO_3 (7.5 mL) and 0.80 g (6 mmol) of 2-tolylboronic acid were added. The mixture was refluxed at 80 °C for 1–2 days until reaction was completed (TLC). After cooling to room temperature, the product was diluted with water and extracted with EtOAc. The organic layers were dried with $MgSO_4$, filtered, and concentrated. Purification was performed by column chromatography using a mixture of CH/EtOAc (9:1). The compounds were used, without structure determination, directly for the next step.

*5.6. General procedure for synthesis of compounds **7a–h** [33]*

To a stirred solution of the appropriately substituted toluene in CCl_4 (10 mL per mmol) were added 0.95 eq. of NBS and AIBN (5 mg per mmol). The reaction mixture was refluxed at 80 °C and then cooled to room temperature. The product was diluted with water and extracted with EtOAc. The organic layers were dried with $MgSO_4$, filtered, and concentrated. Purification was performed by column chromatography using a mixture of CH/EtOAc (6:1). The compounds were used, without structure determination, directly for the next step.

*5.7. General procedure for synthesis of compounds **8a–h**, **9a–f** and **10a–f***

To a solution of compound **4a–c** (0.25 mmol) and 1 N NaOH (0.25 mmol) in DMF (1 mL) was added the appropriate substituted biphenyl system (0.38 mmol) at room temperature, and the mixture was stirred for 5 h. The precipitate formed was collected by filtration and washed once with less DMF and thereafter several times with EtOH to give compounds **8a–h**, **9a–f** and **10a–f**.

Note: The compounds which did not precipitate from the solution were purified as follows. The reaction mixture was diluted with EtOAc and the organic layer was washed with water and brine, dried over $MgSO_4$ and concentrated *in vacuo*. The residue was purified by silica gel column chromatography (DCM/EtOAc – 20:1).

*5.7.1. 2,3-Dihydrobenzo[b][1,4]dioxin-6-yl-5-((2′-nitrobiphenyl-4-yl)methylthio)-1,3,4-oxadiazole (**8a**)*

Yield 77%, yellow solid. ^{1}H NMR (DMSO-d_6, 500 MHz): δ [ppm] = 4.31 (4H, m), 4.63 (2H, s), 7.10 (1H, d, J = 8.4 Hz), 7.35 (2H, m), 7.44 (1H, s), 7.41 (1H, d, J = 8.4 Hz), 7.53 (3H, m), 7.64 (1H, *t*, J = 7.8 Hz), 7.72 (1H, *t*, J = 7.6 Hz), 8.05 (1H, d, J = 8.1 Hz). ^{13}C NMR (DMSO-d_6, 125 MHz): 36.0, 64.5, 64.9, 115.5, 116.4, 118.6, 120.4, 124.5, 128.5, 129.4, 129.9, 132.3, 133.4, 135.0, 136.8, 137.4, 144.3, 147.2, 149.3, 163.1, 165.4. EI-MS: m/z = 447 (M^+).

*5.7.2. 4′-((5-(2,3-Dihydrobenzo[b][1,4]dioxin-6-yl)-1,3,4-oxadiazol-2-ylthio)methyl)-biphenyl-3-carbonitrile (**8b**)*

Yield 36%, colorless solid. ^{1}H NMR (DMSO-d_6, 500 MHz): δ [ppm] = 4.30 (4H, m), 4.62 (2H, s), 7.05 (1H, d, J = 8.5 Hz), 7.39

(1H, d, $J = 2.1$ Hz), 7.44 (1H, dd, $J = 8.5$ Hz, $J = 2.1$ Hz), 7.59 (2H, d, $J = 8.3$ Hz), 7.66 (1H, m), 7.74 (2H, d, $J = 8.3$ Hz), 7.82 (1H, td, $J = 6.6$ Hz, $J = 1.3$ Hz), 8.02 (1H, d, $J = 8.0$ Hz), 8.14 (1H, s). ^{13}C NMR (DMSO-d_6, 125 MHz): δ [ppm] = 36.0, 64.5, 64.9, 112.6, 115.5, 116.4, 118.6, 119.2, 120.4, 127.6, 130.2, 130.6, 130.7, 131.6, 131.9, 137.6, 137.8, 141.1, 144.3, 147.2, 163.0, 165.4. EI-MS: m/z = 427 (M^+). HRMS (EI): m/z calcd for $C_{24}H_{17}N_3O_3S$ 427.0991, found 427.0976.

*5.7.3. 2-(2,3-Dihydrobenzo[b][1,4]dioxin-6-yl)-5-((3′-nitrobiphenyl-4-yl)methylthio)-1,3,4-oxadiazole (**8c**)*

Yield 37%, colorless solid. ^{1}H NMR (DMSO-d_6, 500 MHz): δ [ppm] = 4.32 (4H, m), 4.63 (2H, s), 7.05 (1H, d, $J = 8.1$ Hz), 7.39 (1H, d, $J = 2.1$ Hz), 7.44 (1H, dd, $J = 8.4$ Hz J = 2.1 Hz), 7.62 (2H, d, $J = 8.5$ Hz), 7.77 (3H, m), 8.13 (1H, m), 8.21 (1H, m), 8.42 (1H, m). ^{13}C NMR (DMSO-d_6, 125 MHz): δ [ppm] = 36.0, 64.5, 64.9, 115.5, 116.4, 118.6, 120.4, 121.5, 122.7, 127.7, 130.3, 130.9, 133.7, 137.6, 137.8, 141.7, 144.3, 147.2, 148.9, 163.0, 165.5. EI-MS: m/z = 447 (M^+).

*5.7.4. 4′-((5-(2,3-Dihydrobenzo[b][1,4]dioxin-6-yl)-1,3,4-oxadiazol-2-ylthio)methyl)-biphenyl-4-carbonitrile (**8d**)*

Yield 36%, colorless solid. ^{1}H NMR (DMSO-d_6, 500 MHz): δ [ppm] = 4.33 (4H, m), 4.62 (2H, s), 7.05 (1H, d, $J = 8.3$ Hz), 7.39 (1H, d, $J = 2.1$ Hz), 7.44 (1H, dd, $J = 8.5$ Hz, $J = 2.1$ Hz), 7.61 (2H, d, $J = 8.5$ Hz), 7.74 (2H, d, $J = 8.5$ Hz), 7.90 (4H, m). ^{13}C NMR (DMSO-d_6, 125 MHz): δ [ppm] = 36.0, 64.5, 64.9, 110.6, 115.5, 116.4, 118.6, 119.3, 120.4, 127.7, 128.0, 130.3, 133.3, 138.0, 138.1, 144.3, 144.5, 147.2, 163.0, 165.4. EI-MS: m/z = 427 (M^+).

*5.7.5. 2-(2,3-Dihydrobenzo[b][1,4]dioxin-6-yl)-5-((4′-methoxybiphenyl-4-yl)methylthio)-1,3,4-oxadiazole (**8e**)*

Yield 39%, colorless solid. ^{1}H NMR (DMSO-d_6, 500 MHz): δ [ppm] = 3.87 (3H, s), 4.31 (4H, m), 4.58, (2H, s), 7.01 (2H, d, $J = 8.8$ Hz), 7.04 (1H, d, $J = 8.3$ Hz), 7.43 (2H, m), 7.51 (2H, m), 7.58 (4H, m). ^{13}C NMR (DMSO-d_6, 125 MHz): δ [ppm] = 36.2, 55.6, 64.5, 64.9, 114.8, 115.5, 116.4, 118.6, 120.4, 126.6, 128.2, 130.0, 132.4, 135.5, 139.7, 144.3, 147.1, 159.4, 163.1, 165.4. EI-MS: m/z = 432 (M^+).

*5.7.6. 4′-((5-(2,3-Dihydrobenzo[b][1,4]dioxin-6-yl)-1,3,4-oxadiazol-2-ylthio)methyl)-4-methoxybiphenyl-2-carbonitrile (**8f**)*

Yield 50%, colorless solid. ^{1}H NMR (DMSO-d_6, 500 MHz): δ [ppm] = 3.85 (3H, s), 4.33 (4H, m), 4.64 (2H, s), 7.05 (1H, d, $J = 8.4$ Hz), 7.35 (1H, dd, $J = 8.7$ Hz, $J = 2.8$ Hz), 7.41 (1H, d, $J = 2.0$ Hz), 7.44 (1H, dd, $J = 8.4$ Hz, $J = 2.1$ Hz), 7.53 (4H, m), 7.61 (2H, d, $J = 8.3$ Hz). ^{13}C NMR (DMSO-d_6, 125 MHz): δ [ppm] = 36.0, 56.4, 64.5, 64.9, 111.3, 115.5, 116.4, 118.5, 118.6, 118.8, 120.4, 120.6, 129.3, 129.8, 131.9, 137.0, 137.4, 144.3, 147.2, 159.0, 163.1, 165.4. EI-MS: m/z = 457 (M^+). HRMS (EI): m/z calcd for $C_{25}H_{19}N_3O_4S$ 457.1097, found 457.1122.

*5.7.7. 2-((3′,5′-Difluorobiphenyl-4-yl)methylthio)-5-(2,3-dihydrobenzo[b][1,4]dioxin-6-yl)-1,3,4-oxadiazole (**8g**)*

Yield 41%, colorless solid. ^{1}H NMR (DMSO-d_6, 500 MHz): δ [ppm] = 4.33 (4H, m), 4.61 (2H, s), 7.05 (1H, d, $J = 8.5$ Hz), 7.22 (1H, m), 7.38 (1H, d, $J = 2.1$ Hz), 7.43 (3H, m), 7.57 (2H, d, $J = 8.2$ Hz), 7.73 (2H, d, $J = 8.2$ Hz). ^{13}C NMR (DMSO-d_6, 125 MHz): δ [ppm] = 36.0, 64.5, 64.9, 103.2, 110.1, 110.3, 115.5, 116.4, 118.6, 120.4, 127.5, 130.2, 137.4, 137.9, 143.7, 144.3, 147.2, 162.4, 163.0, 164.3, 165.4. EI-MS: m/z = 438 (M^+).

*5.7.8. 2-(Biphenyl-4-ylmethylthio)-5-(2,3-dihydrobenzo[b][1,4]dioxin-6-yl)-1,3,4-oxadi-azole (**8h**)*

Yield 38%, colorless solid. ^{1}H NMR (DMSO-d_6, 500 MHz): δ [ppm] = 4.31 (4H, m), 4.60 (2H, s), 7.03 (1H, d, $J = 8.4$ Hz), 7.33–7.68 (11H, m). ^{13}C NMR (DMSO-d_6, 125 MHz): δ [ppm] = 36.1, 64.5, 64.9, 115.5, 116.4, 118.6, 120.4, 127.1, 127.3, 127.5, 128.0, 129.4, 130.1, 136.4, 140.1, 144.3, 147.2, 163.1, 165.4. EI-MS: m/z = 402 (M^+).

*5.7.9. 2-(Benzo[d][1,3]dioxol-5-yl)-5-((2′-nitrobiphenyl-4-yl)methylthio)-1,3,4-oxadiazole (**9a**)*

Yield 27%, yellow solid. ^{1}H NMR (DMSO-d_6, 500 MHz): δ [ppm] = 4.62 (2H, s), 6.15 (2H, s), 7.11 (1H, d, $J = 8.13$ Hz), 7.32 (2H, d, $J = 6.4$ Hz), 7.42–7.66 (6H, m), 7.75 (1H, td, $J = 7.6$ Hz, $J = 1.3$ Hz), 7.97 (1H, dd, $J = 8.0$ Hz, $J = 1.2$ Hz). ^{13}C NMR (DMSO-d_6, 125 MHz): δ [ppm] = 36.0, 102.6, 106.6, 109.6, 117.1, 122.2, 124.5, 128.5, 129.4, 129.9, 132.3, 133.4, 135.0, 136.8, 137.3, 148.6, 149.3, 150.9, 163.1, 165.6. EI-MS: m/z = 433 (M^+).

*5.7.10. 4′-((5-(Benzo[d][1,3]dioxol-5-yl)-1,3,4-oxadiazol-2-ylthio)methyl)biphenyl-3-carbo-nitrile (**9b**)*

Yield 41%, off-white. ^{1}H NMR (DMSO-d_6, 500 MHz): δ [ppm] = 4.62 (2H, s), 6.16 (2H, s), 7.11 (1H, d, $J = 8.1$ Hz), 7.43 (1H, d, $J = 1.7$ Hz), 7.51 (1H, dd, $J = 8.2$ Hz, $J = 1.7$ Hz), 7.60 (2H, d, $J = 8.2$ Hz), 7.66 (1H, m), 7.73 (2H, d, $J = 8.2$ Hz), 7.82 (1H, d, $J = 7.7$ Hz), 8.01 (1H, d, $J = 8.0$ Hz), 8.14 (2H, m). ^{13}C NMR (DMSO-d_6, 125 MHz): δ [ppm] = 36.0, 102.5, 106.6, 109.61, 112.5, 117.0, 119.2, 122.1, 127.5, 130.2, 130.5, 130.6, 131.5, 131.8, 137.5, 137.8, 141.1, 148.5, 150.9, 163.0, 165.5. EI-MS: m/z = 413 (M^+). HRMS (EI): m/z calcd for $C_{23}H_{15}N_3O_3S$ 413.0835, found 413.0828.

*5.7.11. 2-(Benzo[d][1,3]dioxol-5-yl)-5-((3′-nitrobiphenyl-4-yl)methylthio)-1,3,4-oxadiazole (**9c**)*

Yield 48%, grey/brown solid. ^{1}H NMR (DMSO-d_6, 500 MHz): δ [ppm] = 4.64 (2H, s), 6.16 (2H, s), 7.11 (1H, d, $J = 8.6$ Hz), 7.44 (1H, d, $J = 1.7$ Hz), 7.52 (1H, dd, $J = 8.1$ Hz, $J = 1.6$ Hz), 7.63 (2H, d, $J = 8.4$ Hz), 7.77 (3H, m), 8.14 (1H, m), 8.22 (1H, m), 8.43 (1H, m). ^{13}C NMR (DMSO-d_6, 125 MHz): δ [ppm] = 36.0, 102.6, 106.6, 109.6, 117.1, 121.5, 122.2, 122.7, 127.7, 130.4, 131.0, 133.7, 137.6, 137.8, 141.4, 148.6, 148.9, 150.9, 163.0, 165.6. EI-MS: m/z = 433 (M^+).

*5.7.12. 2-(Benzo[d][1,3]dioxol-5-yl)-5-((4′-methoxybiphenyl-4-yl)methylthio)-1,3,4-oxadi-azole (**9d**)*

Yield 48%, grey/brown solid. ^{1}H NMR (DMSO-d_6, 500 MHz): δ [ppm] = 3.79 (3H, s), 4.60 (2H, s), 6.16 (2H, s), 7.01 (2H, dd, $J = 2.1$ Hz, $J = 8.8$ Hz), 7.11 (1H, d, $J = 8.2$ Hz), 7.44 (1H, d, $J = 1.8$ Hz), 7.52 (3H, m), 7.59 (4H, m). ^{13}C NMR (DMSO-d_6, 125 MHz): δ [ppm] = 36.2, 53.6, 102.6, 106.6, 109.6, 114.8, 117.1, 122.2, 126.7, 128.2, 130.0, 132.4, 135.5, 139.7, 148.6, 150.9, 159.4, 163.1, 165.5. EI-MS: m/z = 418 (M^+).

*5.7.13. 4′-((5-(Benzo[d][1,3]dioxol-5-yl)-1,3,4-oxadiazol-2-ylthio)methyl)-4-methoxybiphe-nyl-2-carbonitrile (**9e**)*

Yield 47%, off-white. ^{1}H NMR (DMSO-d_6, 500 MHz): δ [ppm] = 3.86 (3H, s), 4.64 (2H, s), 6.16 (2H, s), 7.11 (1H, d, $J = 8.2$ Hz), 7.35(1H, dd, $J = 8.7$ Hz, $J = 2.8$ Hz), 7.45 (1H, d, $J = 1.7$ Hz), 7.52 (5H, m), 7.61 (2H, d, $J = 8.3$ Hz). ^{13}C NMR (DMSO-d_6, 125 MHz): δ [ppm] = 35.9, 56.3, 102.6, 106.6, 109.6, 111.3, 117.1, 118.5, 118.8, 120.6, 122.2, 129.3, 129.8, 131.9, 137.0, 137.3, 137.4, 148.6, 150.9, 159.0, 163.1, 165.6. EI-MS: m/z = 443 (M^+). HRMS (EI): m/z calcd for $C_{24}H_{17}N_3O_4S$ 443.0940, found 443.0902.

*5.7.14. 2-(Benzo[d][1,3]dioxol-5-yl)-5-((3′,5′-difluorobiphenyl-4-yl)methylthio)-1,3,4-oxa-diazole (**9f**)*

Yield 50%, grey/brown solid. ^{1}H NMR (DMSO-d_6, 500 MHz): δ [ppm] = 4.62 (2H, s), 6.16 (2H, s), 7.11 (1H, d $J = 8.1$ Hz), 7.22 (1H, m), 7.44 (3H, m), 7,52 (1H, dd, $J = 8.1$ Hz, $J = 1.8$ Hz), 7.58 (2H, d, $J = 8.3$ Hz), 7.73 (2H, d, $J = 8.3$ Hz). ^{13}C NMR (DMSO-d_6, 125 MHz): δ [ppm] = 35.9, 102.6, 103.2, 106.6, 109.6, 110.1, 110.3, 117.1, 122.2, 127.5, 130.2, 137.4, 137.9, 143.7, 148.6, 150.9, 162.3, 163.0, 164.2, 165.6. EI-MS: m/z = 424 (M^+).

*5.7.15. 2-((2′-Nitrobiphenyl-4-yl)methylthio)-5-(pyridine-4-yl)-1,3,4-oxadiazole (**10a**)*

Yield 79%, yellow solid. ^{1}H NMR (DMSO-d$_6$, 500 MHz): δ [ppm] = 4.7 (2H, s), 7.3 (2H, d, J = 8.2 Hz), 7.5 (1H, d, J = 7.7 Hz), 7.6 (2H, d, J = 8.2 Hz), 7.6 (1H, *t*, J = 7.8 Hz), 7.8 (1H, *t*, J = 7.6 Hz), 7.9 (2H, d, J = 6.1 Hz), 8.0 (1H, d, J = 8.1 Hz), 8.8 (2H, d, J = 6.1 Hz). ^{13}C NMR (DMSO-d$_6$, 125 MHz): δ [ppm] = 36.0, 120.5, 124.6, 128.5, 129.4, 130.0, 130.5, 132.2, 133.4, 135.0, 136.9, 137.2, 149.3, 151.4, 164.3, 165.3. EI-MS: m/z = 390 (M$^+$).

*5.7.16. 4′-((5-(Pyridine-4-yl)-1,3,4-oxadiazol-2-ylthio)methyl) biphenyl-3-carbonitrile (**10b**)*

Yield 53%, yellow solid. ^{1}H NMR (DMSO-d$_6$, 500 MHz): δ [ppm] = 4.68 (2H, s), 7.64 (3H, m), 7.74 (2H, d), 7.82 (1H, dt, J = 7.7 Hz, J = 1.3 Hz), 7.90 (2H, dd, J = 4.5 Hz, J = 1.7 Hz), 8.01 (1H, m), 8.15 (1H, m), 8.82 (2H, dd, J = 4.5 Hz, J = 1.7 Hz). ^{13}C NMR (DMSO-d$_6$, 125 MHz): δ [ppm] = 36.0, 112.6, 119.2, 120.4, 127.6, 130.3, 130.5, 130.6, 130.7, 131.6, 131.9, 137.3, 137.9, 141.1, 151.4, 164.2, 165.2. EI-MS: m/z = 370 (M$^+$).

*5.7.17. 4′-((5-(Pyridine-4-yl)-1,3,4-oxadiazol-2-ylthio)methyl) biphenyl-4-carbonitrile (**10c**)*

Yield 32%, colorless solid. ^{1}H NMR (DMSO-d$_6$, 500 MHz): δ [ppm] = 4.69 (2H, s), 7.64 (2H, d, J = 8.1 Hz), 7.75 (2H, d, J = 8.1 Hz), 7.86-7.93 (6H, m), 8.82 (2H, m). ^{13}C NMR (DMSO-d$_6$, 125 MHz): δ [ppm] = 35.9, 110.6, 119.3, 120.4, 127.8, 128.0, 130.4, 130.5, 133.3, 137.8, 138,1, 144.5, 151.4, 165.2, 164.3. EI-MS: m/z = 370 (M$^+$).

*5.7.18. 2-((4′-Methoxybiphenyl-4-yl)methylthio)-5-(pyridine-4-yl)-1,3,4-oxadiazole (**10d**)*

Yield 37%, colorless solid. ^{1}H NMR (DMSO-d$_6$, 500 MHz): δ [ppm] = 3.79 (3H, s), 4.66 (2H, s), 7.01 (2H, d, J = 8.6 Hz), 7.55 (2H, d, J = 8.2 Hz), 7.60 (4H, m), 7.90 (2H, d, J = 5.8 Hz), 8.82 (2H, d, J = 5.8 Hz). ^{13}C NMR (DMSO-d$_6$, 125 MHz): δ [ppm] = 36.1, 55.6, 114.8, 120.4, 126.8, 128.2, 130.1, 130.5, 132.4, 135.3, 139.8, 151.4, 159.5, 164.2, 165.3. EI-MS: m/z = 375 (M$^+$).

*5.7.19. 4-Fluoro-4′-((5-(pyridine-4-yl)-1,3,4-oxadiazol-2-ylthio) methyl)biphenyl-2-carbonit-rile (**10e**)*

Yield 31%, yellow solid. ^{1}H NMR (DMSO-d$_6$, 500 MHz): δ [ppm] = 4.71 (2H, s), 7.57 (2H, d, J = 1.8 Hz), 7.67 (4H, m), 7.90 (2H, dd, J = 4.4 Hz, J = 1.7 Hz), 7.97 (1H, m), 8.82 (2H, dd, J = 4.4 Hz, J = 1.7 Hz). ^{13}C NMR (DMSO-d$_6$, 125 MHz): δ [ppm] = 35.9, 112.1, 117.9, 120.5, 121.0, 121.5, 129.5, 129.9, 130.5, 132.9, 136.8, 137.8, 141.3, 151.4, 164.3, 165.3. EI-MS: m/z = 388 (M$^+$). HRMS (EI): m/z calcd for $C_{21}H_{13}N_4OFS$ 388.0795, found 388.0825.

*5.7.20. 2-(Biphenyl-4-ylmethylthio)-5-(pyridine-4-yl)-1,3,4-oxadiazole (**10f**)*

Yield 32%, yellow solid. ^{1}H NMR (DMSO-d$_6$, 500 MHz): δ [ppm] = 4.67 (2H, s), 7.36 (1H, m), 7.46 (2H, m), 7.66-7.70 (6H, m), 7.9 (2H, d, J = 6.1 Hz), 8.8 (2H, d, J = 6.1 Hz). ^{13}C NMR (DMSO-d$_6$, 125 MHz): δ [ppm] = 36.1, 120.5, 127.1, 127.3, 128.0, 129.4, 130.2, 130.5, 136.2, 140.0, 140.1, 151.4, 164.1, 165.3. EI-MS: m/z = 345 (M$^+$).

*5.8. Compounds 1**2a**–**d** were prepared in a similar manner to that described for **2a***

The compounds were used, without structure determination, directly for the next step.

*5.9. Compounds **13a**–**d** were prepared in a similar manner to that described for **3a***

The compounds were used, without structure determination, directly for the next step.

*5.10. Compounds **14a**–**d** were prepared in a similar manner to that described for **4a***

The compounds were used, without structure determination, directly for the next step.

*5.11. Compounds **15**–**18** (**a**–**d**) were prepared in a similar manner to that described for compounds **8a**–**h**, **9a**–**f** and **10a**–**f***

*5.11.1. 2-(Benzylthio)-5-phenyl-1,3,4-oxadiazole (**15a**)*

Yield 67%, colorless solid. ^{1}H NMR (DMSO-d$_6$, 500 MHz): δ [ppm] = 4.59 (2H, s), 7.29 (1H, m), 7.35 (2H, m), 7.48 (2H, m), 7.60 (3H, m), 7.95 (2H, m). ^{13}C NMR (DMSO-d$_6$, 125 MHz): δ [ppm] = 35.9, 122.9, 126.3, 127.7, 128.5, 129.0, 129.4, 132.0, 136.5, 163.2, 165.2. EI-MS: m/z = 268 (M$^+$).

*5.11.2. 4′-((5-Phenyl-1,3,4-oxadiazol-2-ylthio)methyl)biphenyl-2-carbonitrile (**15b**)*

Yield 58%, colorless solid. ^{1}H NMR (DMSO-d$_6$, 300 MHz): δ [ppm] = 4.68 (2H, s), 7.53-7.69 (9H, m, br), 7.78 (1H, td, J = 7.7 Hz, J = 1.4 Hz), 7.95 (3H, m). ^{13}C NMR (DMSO-d$_6$, 75 MHz): δ [ppm] = 35.4, 110.0, 118.4, 122.9, 126.3, 128.2, 128.8, 129.3, 130.0, 131.9, 133.4, 133.8, 137.1, 137.3, 143.9, 163.2, 165.2. EI-MS: m/z = 369 (M$^+$).

*5.11.3. 2-(3-Methoxybenzylthio)-5-phenyl-1,3,4-oxadiazole (**15c**)*

Yield 51%, colorless solid. ^{1}H NMR (DMSO-d$_6$, 500 MHz): δ [ppm] = 3.72 (3H, s), 4.55 (2H, s), 6.84 (1H, m), 7.05 (2H, m), 7.26 (1H, *t*, J = 7.8 Hz), 7.62 (3H, m), 7.97 (2H, m). ^{13}C NMR (DMSO-d$_6$, 125 MHz): δ [ppm] = 35.9, 55.0, 113.2, 114.6, 121.1, 122.9, 126.3, 129.4, 129.6, 132.0, 138.0, 159.2, 163.2, 165.2. EI-MS: m/z = 298 (M$^+$).

*5.11.4. 3-((5-Phenyl-1,3,4-oxadiazol-2-ylthio)methyl)benzonitrile (**15d**)*

Yield 38%, colorless solid. ^{1}H NMR (DMSO-d$_6$, 500 MHz): δ [ppm] = 4.63 (2H, s), 7.60 (4H, m), 7.77 (1H, d, J = 7.7 Hz), 7.85 (1H, d, J = 7.9 Hz), 7.94 (2H, m), 7.98 (1H, s). ^{13}C NMR (DMSO-d$_6$, 125 MHz): δ [ppm] = 34.8, 111.3, 118.4, 122.9, 126.3, 129.3, 129.7, 131.4, 132.0, 132.6, 133.9, 138.8, 162.9, 165.3. EI-MS: m/z = 293 (M$^+$).

*5.11.5. 2-(Benzylthio)-5-(4-methoxyphenyl)-1,3,4-oxadiazole (**16a**)*

Yield 63%, colorless solid. ^{1}H NMR (DMSO-d$_6$, 500 MHz): δ [ppm] = 3.85 (3H, s), 4.56 (2H, s), 7.13 (2H, m), 7.28 (1H, m), 7.33 (2H, m), 7.47 (2H, m), 7.89 (2H, m). ^{13}C NMR (DMSO-d$_6$, 125 MHz): δ [ppm] = 35.9, 55.5, 114.8, 115.3, 127.7, 128.2, 128.5, 128.9, 136.6, 162.0, 162.3, 165.1. EI-MS: m/z = 298 (M$^+$).

*5.11.6. 4′-((5-(4-Methoxyphenyl)-1,3,4-oxadiazol-2-ylthio)methyl) biphenyl-2-carbonitrile (**16b**)*

Yield 71%, orange solid. ^{1}H NMR (DMSO-d$_6$, 300 MHz): δ [ppm] = 4.62 (2H, s), 7.22-7.43 (3H, m, br), 7.50 (2H, m), 8.22 (2H, m), 8.41 (2H, m). ^{13}C NMR (DMSO-d$_6$, 75 MHz): δ [ppm] = 35.8, 124.5, 127.7, 127.7, 128.4, 128.5, 129.0, 136.3, 149.1, 163.8, 164.7. EI-MS: m/z = 399 (M$^+$).

*5.11.7. 2-(3-Methoxybenzylthio)-5-(4-methoxyphenyl)-1,3,4-oxadiazole (**16c**)*

Yield 57%, colorless solid. ^{1}H NMR (DMSO-d$_6$, 500 MHz): δ [ppm] = 3.72 (3H, s), 3.85 (3H, s), 4.53 (2H, s), 6.84 (1H, m), 7.03 (2H, *t*, J = 5.0 Hz), 7.13 (2H, m), 7.25 (1H, *t*, J = 7.9 Hz), 7.90 (2H, m).

^{13}C NMR (DMSO-d$_6$, 125 MHz): δ [ppm] = 35.9, 55.0, 55.5, 113.2, 114.6, 114.8, 115.3, 121.1, 128.2, 129.6, 138.0, 159.2, 162.0, 162.4, 165.1. EI-MS: *m*/*z* = 328 (M^+).

*5.11.8. 3-((5-(4-Methoxyphenyl)-1,3,4-oxadiazol-2-ylthio)methyl) benzonitrile (**16d**)*

Yield 41%, colorless solid. ^{1}H NMR (DMSO-d$_6$, 500 MHz): δ [ppm] = 3.84 (3H, s), 4.60 (2H, s), 7.13 (1H, m), 7.57 (2H, *t*, *J* = 7.8 Hz), 7.76 (1H, dt, *J* = 7.7 Hz, *J* = 1.3 Hz), 7.83 (1H, m), 7.88 (2H, m), 7.96 (1H, *t*, *J* = 1.5 Hz). ^{13}C NMR (DMSO-d$_6$, 125 MHz): δ [ppm] = 34.8, 55.5, 111.3, 114.8, 115.2, 118.4, 128.2, 129.7, 131.4, 132.6, 133.9, 138.8, 162.0, 165.3. EI-MS: *m*/*z* = 323 (M^+).

*5.11.9. 4-(5-(Benzylthio)-1,3,4-oxadiazol-2-yl)benzonitrile (**17a**)*

Yield 32%, colorless solid. ^{1}H NMR (DMSO-d$_6$, 300 MHz): δ [ppm] = 4.61 (2H, s), 7.31 (3H, m), 7.49 (2H, d, *J* = 7.3 Hz), 8.09 (4H, td, *J* = 8.2 Hz, *J* = 0.9 Hz). ^{13}C NMR (DMSO-d$_6$, 75 MHz): δ [ppm] = 35.8, 114.0, 118.0, 126.9, 127.0, 127.7, 128.5, 129.0, 133.3, 136.4, 164.0, 164.4. EI-MS: *m*/*z* = 293 (M^+).

*5.11.10. 4′-((5-Phenyl-1,3,4-oxadiazol-2-ylthio)methyl)biphenyl-2-carbonitrile (**17b**)*

Yield 53%, orange solid. ^{1}H NMR (DMSO-d$_6$, 500 MHz): δ [ppm] = 4.72 (2H, s), 7.48 (1H, m), 7.51 (1H, m), 7.57 (2H, m), 7.62 (2H, m), 7.67 (1H, dt, *J* = 7.7 Hz, *J* = 1.3 Hz), 7.79 (1H, dd, *J* = 7.7 Hz, *J* = 0.9 Hz), 7.81 (2H, m), 8.13 (2H, m). ^{13}C NMR (DMSO-d$_6$, 125 MHz): δ [ppm] = 36.4, 111.2, 115.1, 117.8, 118.5, 127.1, 127.4, 127.8, 129.2, 129.5, 129.9, 132.8, 132.9, 133.8, 136.0, 138.0, 144.6, 164.3, 165.1. EI-MS: *m*/*z* = 394 (M^+).

*5.11.11. 4-(5-(3-Methoxybenzylthio)-1,3,4-oxadiazol-2-yl) benzonitrile (**17c**)*

Yield 47%, colorless solid. ^{1}H NMR (DMSO-d$_6$, 500 MHz): δ (ppm) = 3.77 (3H, s), 4.49 (2H, s), 6.82 (1H, dd, *J* = 8.3 Hz, *J* = 2.0 Hz), 6.97 (1H, m), 7.00 (1H, d, *J* = 7.6 Hz), 7.23 (1H, *t*, *J* = 7.9 Hz), 7.75 (2H, m), 8.08 (2H, m). ^{13}C NMR (DMSO-d$_6$, 125 MHz): δ (ppm) = 36.9, 55.3, 113.8, 114.7, 115.1, 117.9, 121.4, 127.1, 127.5, 129.9, 132.9, 136.7, 159.9, 164.3, 165.3. EI-MS: *m*/*z* = 323 (M^+).

*5.11.12. 3-((5-(4-Cyanophenyl)-1,3,4-oxadiazol-2-ylthio)methyl) benzonitrile (**17d**)*

Yield 45%, colorless solid. ^{1}H NMR (DMSO-d$_6$, 300 MHz): δ [ppm] = 4.47 (2H, s), 7.40 (1H, *t*, *J* = 7.8 Hz), 7.52 (1H, m), 7.70 (4H, m), 8.03 (2H, dt, *J* = 6.8 Hz, *J* = 0.9 Hz). ^{13}C NMR (DMSO-d$_6$, 75 MHz): δ [ppm] = 34.9, 112.2, 114.5, 117.1, 117.6, 126.4, 126.5, 129.0, 131.1, 131.9, 132.2, 133.0, 136.8, 163.8, 163.9. EI-MS: *m*/*z* = 318 (M^+).

*5.11.13. 2-(Benzylthio)-5-(4-nitrophenyl)-1,3,4-oxadiazole (**18a**)*

Yield 46%, light yellow solid. ^{1}H NMR (DMSO-d$_6$, 300 MHz): δ [ppm] = 4.62 (2H, s), 7.32 (3H, m), 7.49 (2H, m), 8.21 (2H, m), 8.41 (2H, m). ^{13}C NMR (DMSO-d$_6$, 75 MHz): δ [ppm] = 35.8, 124.5, 127.7, 127.7, 128.4, 128.5, 129.0, 136.3, 149.1, 163.8, 164.7. EI-MS: *m*/*z* = 313 (M^+).

*5.11.14. 4′-((5-(4-Nitrophenyl)-1,3,4-oxadiazol-2-ylthio)methyl) biphenyl-2-carbonitrile (**18b**)*

Yield 58%, orange solid. ^{1}H NMR (DMSO-d$_6$, 500 MHz): δ [ppm] = 4.71 (2H, s), 7.60 (4H, m), 7.68 (2H, d, *J* = 8.2 Hz), 7.78 (1H, dt, *J* = 7.7 Hz, *J* = 1.2 Hz), 7.94 (1H, dd, *J* = 7.7 Hz, *J* = 0.9 Hz), 8.22 (2H, m), 8.41 (2H, m). ^{13}C NMR (DMSO-d$_6$, 125 MHz): δ [ppm] = 35.9, 110.5, 118.9, 125.0, 128.2, 128.7, 129.0, 129.4, 129.9, 130.5, 134.0, 134.3, 137.7, 137.7, 144.4, 149.6, 164.4, 165.2. EI-MS: *m*/*z* = 414 (M^+).

*5.11.15. 2-(3-Methoxybenzylthio)-5-(4-nitrophenyl)1,3,4-oxadiazole (**18c**)*

Yield 33%, yellow solid. ^{1}H NMR (DMSO-d$_6$, 500 MHz): δ (ppm) = 3.73 (3H, s), 4.59 (2H, s), 6.86 (1H, m), 7.07 (2H, m), 7.27 (1H, *t*, *J* = 7.9 Hz), 8.23 (2H, m), 8.40 (2H, m). ^{13}C NMR (DMSO-d$_6$, 125 MHz): 35.8, 55.0, 113.3, 114.6, 121.2, 124.5, 127.7, 128.4, 129.7, 137.8, 149.1, 159.2, 163.9, 154.7. EI-MS: *m*/*z* = 343 (M^+).

*5.11.16. 3-((5-(4-Nitrophenyl)-1,3,4-oxadiazol-2-ylthio)methyl) benzonitrile (**18d**)*

Yield 47%, orange solid. ^{1}H NMR (DMSO-d$_6$, 300 MHz): δ [ppm] = 4.66 (2H, s), 7.58 (1H, *t*, *J* = 7.8 Hz), 7.76 (1H, m), 7.86 (1H, m), 7.99 (1H, dd, *J* = 2.3 Hz, *J* = 1.1 Hz), 8.20 (2H, m), 8.41 (2H, m). ^{13}C NMR (DMSO-d$_6$, 75 MHz): δ [ppm] = 34.7, 111.3, 118.4, 124.5, 127.7, 128.4, 129.7, 131.4, 132.6, 134.0, 138.6, 149.1, 164.0, 164.4. EI-MS: *m*/*z* = 338 (M^+).

*5.12. General procedure for synthesis of compounds **20a**–**d** [52]*

The appropriate benzaldehyde (1.0 eq.) was dissolved in 5 mL EtOH and isoniazid (1.0 eq.) was added slowly to the solution. The reaction mixture was stirred at room temperature for 16 h. The solvent was removed under vacuum and the residue was purified by recrystallization in EtOH.

*5.12.1. (E)-N′-benzylideneisonicotinohydrazide (**20a**)*

Yield 85%, colorless solid. ^{1}H NMR (DMSO-d$_6$, 500 MHz): δ [ppm] = 7.47 (3H, m), 7.76 (2H, m), 7.83 (2H, dd, *J* = 4.3 Hz, *J* = 1.5 Hz), 8.47 (1H, s), 8.79 (2H, dd, *J* = 4.5 Hz, *J* = 1.5 Hz), 12.09 (1H, s). ^{13}C NMR (DMSO-d$_6$, 125 MHz): δ [ppm] = 121.4, 127.1, 128.7, 130.2, 133.9, 140.3, 148.9, 150.2, 161.5. EI-MS: *m*/*z* = 225 (M^+).

*5.12.2. (E)-N′-(4-Methoxybenzylidene)isonicotinohydrazide (**20b**)*

Yield 97%, yellow solid. ^{1}H NMR (DMSO-d$_6$, 500 MHz): δ [ppm] = 3.83 (3H, s), 7.03 (2H, d, *J* = 9.0 Hz), 7.70 (2H, d, *J* = 9.0 Hz), 7.81 (2H, dd, *J* = 4.5 Hz, *J* = 1.5 Hz), 8.42 (1H, s), 8.78 (2H, dd, *J* = 4.5 Hz, *J* = 1.5 Hz), 11.93 (1H, s). ^{13}C NMR (DMSO-d$_6$, 125 MHz): δ [ppm] = 55.24, 114.31, 121.3, 126.4, 128.2, 140.5, 148.8, 150.2, 161.0, 161.3. EI-MS: *m*/*z* = 255 (M^+).

*5.12.3. (E)-N′-(4-Cyanobenzylidene)isonicotinohydrazide (**20c**)*

Yield 83%, colorless solid. ^{1}H NMR (DMSO-d$_6$, 500 MHz): δ [ppm] = 7.83 (2H, dd, *J* = 4.3 Hz, *J* = 1.5 Hz), 7.94 (4H, s), 8.51 (1H, s), 8.80 (2H, dd, *J* = 4.5 Hz, *J* = 1.5 Hz), 12.27 (1H, s). ^{13}C NMR (DMSO-d$_6$, 125 MHz): δ [ppm] = 112.1, 118.4, 121.4, 127.7, 128.3, 132.6, 140.0, 146.9, 150.2, 161.8. EI-MS: *m*/*z* = 250 (M^+).

*5.12.4. (E)-N′-(4-Ethylbenzylidene)isonicotinohydrazide (**20d**)*

Yield 96%, colorless solid. ^{1}H NMR (DMSO-d$_6$, 500 MHz): δ [ppm] = 1.20 (3H, *t*, *J* = 7.5 Hz), 2.65 (2H, m), 7.32 (2H, d, *J* = 8.1 Hz), 7.67 (2H, d, *J* = 8.1 Hz), 7.82 (2H, dd, *J* = 4.5 Hz, *J* = 1.8 Hz), 8.44 (1H, s), 8.78 (2H, dd, *J* = 4.5 Hz, *J* = 1.8 Hz), 11.99 (1H, s). ^{13}C NMR (DMSO-d$_6$, 125 MHz): δ [ppm] = 15.2, 28.0, 121.4, 127.2, 128.2, 131.4, 140.4, 146.4, 149.0, 150.2, 161.4. EI-MS: *m*/*z* = 253 (M^+).

*5.13. Compound **22** was prepared in a similar manner to that described for **2a***

Methyl 2-aminoisonicotinate (**22**). Yield 89%, colorless solid. ^{1}H NMR (DMSO-d$_6$, 500 MHz): δ [ppm] = 3.84 (3H, s), 6.28 (2H, s), 6.87 (1H, dd, *J* = 5.2 Hz, *J* = 1.5 Hz), 6.96 (1H, m), 8.05 (1H, dd, *J* = 5.2 Hz, *J* = 0.6 Hz). ^{13}C NMR (DMSO-d$_6$, 125 MHz): δ [ppm] = 52.4, 107.4, 110.0, 137.8, 148.9, 160.5, 165.7. EI-MS: *m*/*z* = 152 (M^+).

5.14. Methyl 2-acetamidoisonicotinate (**23**)

A solution of compound **22** (760 mg, 5 mmol) in acetic anhydride (20 mL) was heated at 80 °C for 6 h. The reaction was cooled to room temperature and the precipitate formed was filtered off and well washed with water to obtain compound **23** (0.67 g, 69%)as yellow solid. ^{1}H NMR (DMSO-d_6, 500 MHz): δ [ppm] = 2.12 (3H, s), 3.89 (3H, s), 7.52 (1H, dd, J = 5.0 Hz, J = 1.4 Hz), 8.48 (1H, d, J = 5.0 Hz), 8.57 (1H, s), 10.74 (1H, s). ^{13}C NMR (DMSO-d_6, 125 MHz): δ [ppm] = 23.8, 52.7, 112.2, 117.9, 138.6, 149.0, 153.0, 165.1, 169.6. EI-MS: m/z = 154 (M^+).

5.15. Compound **24** was prepared in a similar manner to that described for **3a**

N-(4-(Hydrazinecarbonyl)pyridin-2-yl)acetamide (**24**). Yield 74%, light yellow solid. ^{1}H NMR (DMSO-d_6, 500 MHz): δ [ppm] = 2.11 (3H, s), 4.58 (2H, s), 7.38 (1H, dd, J = 5.1 Hz, J = 1.5 Hz), 8.38 (1H, dd, J = 5.1 Hz, J = 0.7 Hz), 8.41 (1H, s), 9.99 (1H, s), 10.59 (1H, s). ^{13}C NMR (DMSO-d_6, 125 MHz): δ [ppm] = 23.9, 111.3, 116.2, 142.8, 148.2, 152.7, 164.2, 169.3. EI-MS: m/z = 194 (M^+).

5.16. Compound **25** was prepared in a similar manner to that described for **4a**

N-(4-(5-Mercapto-1,3,4-oxadiazol-2-yl)pyridin-2-yl)acetamide (**25**). Yield 92%, yellow solid. ^{1}H NMR (DMSO-d_6, 500 MHz): δ [ppm] = 2.14 (3H, s), 7.49 (1H, dd, J = 5.1 Hz, J = 1.5 Hz), 8.53 (1H, dd, J = 5.1 Hz, J = 0.7 Hz), 8.54 (1H, s), 10.82 (1H, s), 14.90 (1H, s). ^{13}C NMR (DMSO-d_6, 125 MHz): δ [ppm] = 23.9, 108.8, 114.9, 131.4, 149.4, 153.0, 158.8, 169.8, 177.7. EI-MS: m/z = 236 (M^+).

5.17. Compounds **26a–d** were prepared in a similar manner to that described for compounds **8a–h, 9a–f** and **10a–f**

5.17.1. N-(4-(5-(Benzylthio)-1,3,4-oxadiazol-2-yl)pyridin-2-yl) acetamide (**26a**)

Yield 68%, colorless solid. ^{1}H NMR (DMSO-d_6, 500 MHz): δ [ppm] = 2.15 (3H, s), 4.61 (2H, s), 7.30 (1H, m), 7.36 (2H, m), 7.51 (2H, m), 7.58 (1H, dd, J = 5.1 Hz, J = 1.5 Hz), 8.52 (1H, dd, J = 5.1 Hz, J = 0.8 Hz), 8.63 (1H, s), 10.80 (1H, s). ^{13}C NMR (DMSO-d_6, 125 MHz): δ [ppm] = 24.0, 35.9, 109.2, 115.4, 127.8, 128.6, 129.1, 131.7, 136.4, 149.4, 153.0, 163.8, 164.4, 169.8. EI-MS: m/z = 326 (M^+).

5.17.2. **N**-(4-(5-(3-Methoxybenzylthio)-1,3,4-oxadiazol-2-yl) pyridin-2-yl)acetamide (**26b**)

Yield 51%, yellow solid. ^{1}H NMR (DMSO-d_6, 500 MHz): δ [ppm] = 2.14 (3H, s), 3.73 (3H, s), 4.58 (2H, s), 6.86 (1H, m), 7.07 (2H, m), 7.27 (1H, m), 7.58 (1H, dd, J = 5.1 Hz, J = 1.5 Hz), 8.52 (1H, dd, J = 5.1 Hz, J = 0.7 Hz), 8.63 (1H, s), 10.80 (1H, s). ^{13}C NMR (DMSO-d_6, 125 MHz): δ [ppm] = 24.0, 35.9, 55.0, 109.2, 113.3, 114.6, 115.4, 121.2, 129.7, 131.8, 137.8, 149.4, 153.0, 159.3, 163.8, 164.7, 169.8. EI-MS: m/z = 356 (M^+).

5.17.3. **N**-(4-(5-(Benzylthio)-1,3,4-oxadiazol-2-yl)pyridin-2-yl) acetamide (**26c**)

Yield 37%, colorless solid. ^{1}H NMR (DMSO-d_6, 500 MHz): δ [ppm] = 2.14 (3H, s), 4.64 (2H, s), 7.57 (2H, m), 7.77 (1H, d, J = 7.8 Hz), 7.87 (1H, d, J = 7.8 Hz), 7.97 (1H, s), 8.51 (1H, d, J = 5.1 Hz), 8.61 (1H, s), 10.81 (1H, s). ^{13}C NMR (DMSO-d_6, 125 MHz): δ [ppm] = 23.9, 34.8, 109.2, 111.4, 115.4, 118.5, 129.8, 131.5, 131.8, 132.6, 134.1, 138.6, 149.5, 153.0, 163.9, 164.4, 169.8. EI-MS: m/z = 351 (M^+). HRMS (EI): m/z calcd for $C_{17}H_{13}N_5O_2S$ 351.0791, found 351.0787.

5.17.4. N-(4-(5-((2′-Cyanobiphenyl-4-yl)methylthio)-1,3,4-oxadiazol-2-yl)pyridin-2-yl)acet-amide (**26d**)

Yield 62%, light yellow solid. ^{1}H NMR (DMSO-d_6, 500 MHz): δ [ppm] = 2.14 (3H, s), 4.70 (2H, s), 7.56-7.61 (5H, m), 7.68 (2H, d, J = 8.2 Hz), 7.78 (1H, td, J = 7.6 Hz, J = 1.3 Hz), 7.94 (1H, dd, J = 7.6 Hz, J = 1.1 Hz), 8.52 (1H, dd, J = 5.1 Hz, J = 0.7 Hz), 8.64 (1H, s), 10.80 (1H, s). ^{13}C NMR (DMSO-d_6, 125 MHz): δ [ppm] = 23.9, 35.5, 109.3, 110.1, 115.4, 118.5, 128.3, 128.9, 129.4, 130.1, 131.8, 133.5, 133.9, 137.2, 144.0, 149.5, 153.1, 163.9, 164.7, 169.8. EI-MS: m/z = 427 (M^+). HRMS (EI): m/z calcd for $C_{23}H_{17}N_5O_2S$ 427.1104, found 427.1104.

5.18. Ethyl 4-aminobenzoate (**28**)

To a solution of compound **27** (3.4 g, 25 mmol) in ethanol (30 mL) was added dropwise concentrated sulfuric acid (2.4 mL). The mixture was heated under reflux for 6 h. The resulting solution was diluted with water (200 mL) and made neutral by addition of concentrated ammonia water. The precipitation was collected by filtration and then washed with water and subsequently dried to afford compound **28** (3.68 g, 91%) as colorless solid. The compound was used, without structure determination, directly for the next step.

5.19. Ethyl 2-aminobenzo[d]thiazole-6-carboxylate (**29**)

Compound **28** (2.0 g, 12 mmol) was dissolved in 16 mL of acetic acid, and to the resulting solution was suspended potassium thiocyanate (4.67 g, 48 mmol). A solution of 0.61 mL of bromine in 8 ml of acetic acid was slowly added, and the reaction mixture was stirred at room temperature overnight. Water was added and the mixture was made neutral by addition of aqueous ammonium hydroxide. The precipitation was collected by filtration and then washed with water and subsequently dried to afford compound **29** (1.80 g, 67%) as light yellow solid. The compound was used, without structure determination, directly for the next step.

5.20. Compound **30** was prepared in a similar manner to that described for **23**

Ethyl 2-acetamidobenzo[*d*]thiazole-6-carboxylate (**30**). Yield 58%, light brown solid. The compound was used, without structure determination, directly for the next step.

5.21. 2-Acetamidobenzo[d]thiazole-6-carboxylic acid (**31**)

A solution of compound **30** (1.0 g, 3.8 mmol), 1 N NaOH (40 mL), and MeOH (15 mL) was stirred at room temperature for 4 h and then the solvent was evaporated. To the resulting aqueous layer was added water (10 mL) and the solution acidified with 1 N HCl to pH 2. The resulting solid was collected by filtration and washed with water. The solid was dried to afford compound **31** (0.84 g, 94%) as light brown solid. The compound was used, without structure determination, directly for the next step.

5.22. N-(6-(2-tert-Butylhydrazinecarbonyl)benzo[d]thiazol-2-yl) acetamide (**32**)

To a solution of **31** (0.80 g, 3.3 mmol), *tert*-butyl carbazate (0.47 g, 3.6 mmol) and 1-(3-dimethylaminopropyl)-3-ethylcarbodiimide hydrochloride (EDCI) (0.74 g, 3.9 mmol) in DMF (10 mL) was added 1-hydroxybenzotriazole hydrate (HOBt•H_2O) (0.59 g, 3.9 mmol) and the mixture stirred overnight at room temperature. The reaction mixture was diluted with EtOAc and the organic layer was washed with water and brine, dried over

Na_2SO_4 and concentrated *in vacuo*. The residue was recrystallized in EtOAc/CH to give **32** (0.79 g, 77%) as light brown solid. The compound was used, without structure determination, directly for the next step.

5.23. N-(6-(Hydrazinecarbonyl)benzo[d]thiazol-2-yl)acetamide (**33**)

A solution of **32** (0.75 g, 2.4 mmol) in trifluoroacetic acid (5 mL) was stirred at room temperature for 1 h. The solvent was concentrated to give **33** (0.59 g, 99%) as colorless solid. The compound was used, without structure determination, directly for the next step.

5.24. Compound **34** was prepared in a similar manner to that described for **4a**

5.24.1. N-(6-(5-Mercapto-1,3,4-oxadiazol-2-yl)benzo[d]thiazol-2-yl)acetamide (**34**)

Yield 81%, light brown solid. The compound was used, without structure determination, directly for the next step.

5.25. Compounds **35** was prepared in a similar manner to that described for compounds **8a**–**h**, **9a**–**f** and **10a**–**f**

5.25.1. N-(6-(5-((2′-Cyanobiphenyl-4-yl)methylthio)-1,3,4-oxadiazol-2-yl)benzo[d]thiazol-2-yl)acetamide (**35**)

Yield 47%, light brown solid. ^{1}H NMR (DMSO-d_6, 500 MHz): δ [ppm] = 2.23 (3H, s), 4.69 (2H, s), 7.59 (4H, m), 7.67 (2H, d, J = 8.3 Hz), 7.78 (1H, td, J = 7.7 Hz, J = 1.4 Hz), 7.88 (1H, d, J = 8.5 Hz), 7.94 (1H, dd, J = 7.8 Hz, J = 1.1 Hz), 8.01 (1H, dd, J = 8.5 Hz, J = 1.8 Hz), 8.64 (1H, d, J = 1.5 Hz), 12.56 (1H, s). ^{13}C NMR (DMSO-d_6, 125 MHz): δ [ppm] = 22.7, 35.5, 110.0, 117.8, 118.4, 120.6, 121.0, 124.3, 128.2, 128.9, 129.4, 130.0, 132.4, 133.5, 133.8, 137.1, 137.3, 143.9, 151.1, 160.7, 162.9, 165.4, 169.7. EI-MS: m/z = 483 (M^+).

5.26. Methyl 3-bromo-4-hydroxybenzoate (**37**)

To a solution of **36** (3.15 g, 20.7 mmol) in DCM (230 mL) was added slowly at −5 °C a solution of bromine (1.1 mL, 21 mmol) in DCM (50 mL). The mixture was stirred for 4.5 h at room temperature. The reaction mixture was diluted with EtOAc and the organic layer was washed with water and brine, dried over $MgSO_4$ and concentrated *in vacuo*. The residue was purified by silica gel column chromatography (DCM/EtOAc) to give **37** (3.10 g, 65%) as colorless solid. The compound was used, without structure determination, directly for the next step.

5.27. Methyl 8-nitrodibenzo[b,d]furan-2-carboxylate (**38**)

A mixture of compound **37** (0.51 g, 2.2 mmol), 1-fluoro-4-nitrobenzene (0.36 g, 2.2 mmol) and Palladium(II) acetate (0.05 g, 0.22 mmol) in *N*,*N*-dimethylacetamide (2 mL) was stirred overnight at 130 °C. The reaction mixture was diluted with EtOAc (20 mL) and filtered over celite. The solvent was removed *in vacuo* and the resulting oil was diluted with water (7 mL). The precipitate formed was collected by filtration and recrystallized in EtOH to give compound **38** (0.18 g, 30%) as colorless solid. The compound was used, without structure determination, directly for the next step.

5.28. 8-Nitrodibenzo[b,d]furan-2-carbohydrazide (**39**)

To compound **38** (160 mg, 0.59 mmol) was added hydrazine hydrate (1.5 mL) and the mixture was heated at reflux for 6 h. After cooling to room temperature pure crystals are formed, collected by filtration and washed several times with EtOH to give compound **39** (158 mg, 99%) as a yellow solid. The compound was used, without structure determination, directly for the next step.

5.29. Compound **40** was prepared in a similar manner to that described for **4a**

5-(8-Nitrodibenzo[*b*,*d*]furan-2-yl)-1,3,4-oxadiazole-2-thiol (**40**). Yield 48%, light brown solid. The compound was used, without structure determination, directly for the next step.

5.30. Compound **41** was prepared in a similar manner to that described for compounds **8a**–**h**, **9a**–**f** and **10a**–**f**

5.30.1. 3-({[5-(8-Nitrodibenzo[b,d]furan-2-yl)-1,3,4-oxadiazol-2-yl] sulfanyl}methyl)benzonitril (**41**)

Yield 44%, yellow solid. ^{1}H NMR (DMSO-d_6, 500 MHz): δ [ppm] = 4.71 (2H, s), 7.63 (1H, *t*, J = 7.8 Hz), 7.81 (1H, m), 7.96 (1H, m), 8.03 (3H, m), 8.25 (1H, d, J = 8.7 Hz), 8.58 (1H, d, J = 9.1 Hz), 9.11 (1H, s), 9.42 (1H, s). ^{13}C NMR (DMSO-d_6, 125 MHz): δ [ppm] = 35.7, 64.5, 114.0, 119.7, 122.3, 125.0, 128.3, 130.7, 132.4, 133.6, 134.9. EI-MS: m/z = 428 (M^+).

5.31. Determination of GSK-3 inhibition

GSK-3β in vitro assay: Purified GSK-3β (0.5 μg) was incubated in a reaction mixture of 50 mM Tris pH 7.3, 10 mM MgAc, 0.01% β-mercaptoethanol, ^{32}P[γ-ATP](100 μM, 0.5 μci/assay), and 100 μM of peptide substrate, pIRS-1 (RREGGMSRPAS(p)VDG). New molecules were added at various concentrations (1, 10 and 100 μM), and the reaction mixture was incubated for 15 min at 30 °C. The reactions were stopped, spotted on p81 paper (Whatman), washed with 10 mM phosphoric acid, and counted for radioactivity [53].GSK-3β activity was calculated as the percentage of GSK-3β activity in the absence of inhibitors that was designated to 100%.

Kinase Panel: Compounds are serially diluted 1/3 in neat DMSO (10 serial dilutions) and these dilutions are further diluted 1/25 with reaction buffer. 2.5 μL of these solutions are added to the reaction mixture described below so that final compound concentration in the assay ranges from 100 μM to 5 nM in 1% (v/v) DMSO. The enzymatic activity of the kinases is determined with a commercial system based on the Z′-LYTE® technology, available from Invitrogen Life Technologies (Carlsbad, CA, USA), using human recombinant kinases as the enzyme source.

Kinase	Enzyme conc. (nM)	ATP conc. (μM)	Peptide used	Peptide conc. (μM)	Buffer
GSK-3β	2	12.5	Ser/Thr 9 peptide	2	50 mM Hepes pH 7.5, 10 mM $MgCl_2$, 1 mM EGTA, 0.01% (w/v) Brij-35
GSK-3α	0.5	12.5	Ser/Thr 9 peptide	2	“
CKIε	12	32	Ser/Thr 11 peptide	2	“
Cdk5	10	12.5	Ser/Thr 12 peptide	2	“
AurKA	20	10	Ser/Thr 1 peptide	2	“
PKCα	0.15	10	Ser/Thr 7 peptide	2	“

This technology utilizes the fluorescence resonance energy transfer ("FRET") process between fluorescein and coumarin. The assay principle is based on the differential sensitivity of phosphorylated and non-phosphorylated peptide to proteolytic cleavage, which precludes the energy transfer process between the two fluorophores attached to both sides of the cleavage site. Hence, enzymatic phosphorylation will yield a phosphopeptide, which cannot be hydrolyzed by a suitable protease and energy transfer between the two fluorophores will occur. Opposingly, lack of phosphorylation will cause peptide hydrolysis hence lack of energy transfer as. The assay is performed in 96-well black plates, in a final volume of 10 μL.

5.32. Determination of the in vivo activity on wt zebrafish embryos

In Vivo Activity on Zebrafish Embryos: The wt zebrafish was used in this study. The embryos were collected and placed into 24-well plates, ten embryos per well and maintained in E2 medium at ~28 °C. Compounds were added 5 hpf (50% epiboly) and the embryos allowed to grow in chemical compound solution up to 2 days. The phenotypes were compared using the Axio Scope.A1 microscope system from Carl Zeiss at 44–48 hpf [49,50,54].

5.33. Docking simulations

Molecular docking of **9e** and **26d** into the X-ray structure of GSK-3β (PDB code: 3F88) was carried out using Molegro Virtual Docker 5.

Acknowledgments

This work was supported by a collaborative project financed by the 7th Framework Program of the European Union: NeuroGSK3.

Appendix A. Supplementary information

Supplementary data related to this article can be found online at http://dx.doi.org/10.1016/j.ejmech.2012.06.006.

References

[1] F. Lo Monte, T. Kramer, A. Boländer, B. Plotkin, H. Eldar-Finkelman, A. Fuertes, J. Dominguez, B. Schmidt, Synthesis and biological evaluation of glycogen synthase kinase 3 (GSK-3) inhibitors: an fast and atom efficient access to 1-aryl-3-benzylureas, Bioorg. Med. Chem. Lett. 21 (2011) 5610–5615.
[2] C. Hooper, R. Killick, S. Lovestone, The GSK3 hypothesis of Alzheimer's disease, J. Neurochem. 104 (2008) 1433–1439.
[3] A. Alzheimer, Über eine eigenartige Erkankung der Hirnrinde, Allgemeine Zeitschrift Für Psychiatrie Und Psychisch-gerichtliche Medizin (Berlin) 64 (1907) 146–148.
[4] A. Alzheimer, R.A. Stelzmann, H.N. Schnitzlein, F.R. Murtagh, An English translation of Alzheimer's 1907 paper, "Über eine eigenartige Erkankung der Hirnrinde", Clin. Anat. 8 (1995) 429–431.
[5] P. Cohen, M. Goedert, GSK3 inhibitors: development and therapeutic potential, Nat. Rev. Drug Discov. 3 (2004) 479–487.
[6] F. Hernández, J. Avila, The role of glycogen synthase kinase 3 in the early stages of Alzheimers' disease, FEBS Lett. 582 (2008) 3848–3854.
[7] Eldar-Finkelman, Glycogen synthase kinase 3: an emerging therapeutic target, Trends Mol. Med. 8 (2002) 126–132.
[8] M. Mazanetz, P. Fischer, Untangling tau hyperphosphorylation in drug design for neurodegenerative diseases, Nat. Rev. Drug Discov. 6 (2007) 464–479.
[9] L. Chico, L. Van Eldik, D. Watterson, Targeting protein kinases in central nervous system disorders. 892–909, Nat. Rev. Drug Discov. 8 (2009).
[10] L. Meijer, M. Flajolet, P. Greengard, Pharmacological inhibitors of glycogen synthase kinase 3, TRENDS. Pharmacol. Sci. 25 (2004) 471–480.
[11] A. Martinez, C. Gil, D.I. Perez, Glycogen synthase kinase 3 inhibitors in the next horizon for Alzheimer's disease treatment, Int. J. of Alzheimer's Disease 2011 (2011) 1–7.
[12] K.F. Lau, C.C.J. Miller, B.H. Anderton, P.C. Shaw, Expression analysis of glycogen synthase kinase-3 in human tissues, J. Pept. Res. 54 (1999) 85–91.
[13] S. Frame, P. Cohen, GSK3 takes centre stage more than 20 years after its discovery, Biochem. J. 359 (2001) 1–16.
[14] E. Hur, F. Zhou, GSK3 signalling in neural development, Nat. Rev. Neurosci. 11 (2010) 539–551.
[15] F. Mukai, K. Ishiguro, Y. Sano, S.C. Fujita, Alternative splicing isoform of tau protein kinase I/glycogen synthase kinase 3 beta, J. Neurochem. 81 (2002) 1073–1083.
[16] E. ter Haar, J.T. Coll, D.A. Austen, H. Hsiao, L. Swenson, J. Jain, Structure of GSK3β reveals a primed phosphorylation mechanism, Nat. Struct. Biol. 8 (2001) 593–596.
[17] R. Dajani, E. Fraser, S.M. Roe, N. Young, V. Good, T.C. Dale, L.H. Pearl, Crystal structure of glycogen synthase kinase 3: structural basis for phosphate-primed substrate specificity and autoinhibition, Cell 105 (2001) 721–732.
[18] A. Takashima, Drug development targeting the glycogen synthase kinase-3β (GSK-3β)-mediated signal transduction pathway: role of GSK-3β in adult brain, J. Pharmacol. Sci. 109 (2009) 174–178.
[19] L. Serenó, M. Coma, M. Rodriguez, P. Sánchez-Ferrer, M.B. Sánchez, I. Gich, J.M. Agulló, J. Avila, M. Pérez, C. Guardia-Laguarta, J. Clarimón, A. Lleó, T. Gómez-Isla, A novel GSK-3β inhibitor reduces Alzheimer's pathology and rescues neuronalloss in vivo, Neurobiol. Dis. 35 (2009) 359–367.
[20] H. Yamaguchi, K. Ishiguro, T. Uchida, A. Takashima, C.A. Lemere, K. Imahori, Preferential labeling of Alzheimer neurofibrillary tangles with antisera for tau protein kinase (TPK) I/glycogen synthase kinase-3β and cyclin-dependent kinase 5, a component of TPK II, Acta Neuropathol. 92 (1996) 232–241.
[21] A. Martinez, A. Castro, I. Dorronsoro, M. Alonso, Glycogen synthase kinase 3 (GSK-3) inhibitors as new promising drugs for diabetes, neurodegeneration, cancer, and inflammation, Med. Res. Rev. 22 (2002) 373–384.
[22] L. Feng, Y. Geisselbrecht, S. Blanck, A. Wilbuer, G.E. Atilla-Gokcumen, P. Filippakopoulos, K. Krling, M.A. Celik, K. Harms, J. Maksimoska, R. Marmorstein, G. Frenking, S. Knapp, L. Essen, E. Meggers, Structurally sophisticated octahedral metal complexes as highly selective protein kinase inhibitors, J. Am. Chem. Soc. 133 (2011) 5976–5986.
[23] R.V. Bhat, S.L. Budd Haeberlein, J. Avila, Glycogen synthase kinase 3: a drug target for CNS therapies, J. Neurochem. 89 (2004) 1313–1317.
[24] F. Lo Monte, T. Kramer, J. Gu, U. Rao Anumala, L. Marinelli, V. La Pietra, E. Novellino, B. Franco, D. Demedts, F. Van Leuven, A. Fuertes, J.M. Dominguez, B. Plotkin, H. Eldar-Finkelman, B. Schmidt, Identification of glycogen synthase Kinase-3 inhibitors with a selective sting for glycogen synthase Kinase-3α, J. Med. Chem. 55 (2012) 4407–4424.
[25] T. Kramer, B. Schmidt, F. Lo Monte, Small-molecule inhibitors of GSK-3-Structural insights and their application to Alzheimer's disease models, Int. J. of Alzheimer's Disease (2012). accepted, http://www.hindawi.com/journals/ijad/aip/381029/.
[26] B. Voigt, M. Krug, C. Schächtele, F. Totzke, A. Hilgeroth, Probing novel 1-Aza-9-oxafluorenes as selective GSK-3β inhibitors, ChemMedChem 3 (2008) 120–126.
[27] J. Boström, A. Hogner, A. Llinás, E. Wellner, A.T. Plowright, Oxadiazoles in medicinal chemistry, J. Med. Chem. 55 (2012) 1817–1830.
[28] M. Saitoh, J. Kunitomo, E. Kimura, Y. Hayase, H. Kobayashi, N. Uchiyama, T. Kawamoto, T. Tanaka, C.D. Mol, D.R. Dougan, G.S. Textor, G.P. Snell, F. Itoh, Design, synthesis and structure–activity relationships of 1,3,4-oxadiazole derivatives as novel inhibitors of glycogen synthase kinase-3β, Bioorg. Med. Chem. 17 (2009) 2017–2029.
[29] L. Naerum, L. Norskov-Lauritsen, P.H. Olesen, Scaffold hopping and optimization towards libraries of glycogen synthase kinase-3 inhibitors, Bioorg. Med. Chem. Lett. 12 (2002) 1525–1528.
[30] R. Bhat, X. Xue, S. Berg, S. Hellberg, M. Ormö, Y. Nilsson, A. Radesäter, E. Jerning, P. Markgren, M. Nylöf, T. Borgegard, A. Giménez-Cassina, F. Hernández, J.J. Lucas, J. Díaz-Nido, J. Avila, Structural insights and biological effects of glycogen synthase kinase 3-specific inhibitor AR-A014418, J. Biol. Chem. 278 (2003) 45937–45945.
[31] H.B. Konig, W. Seifken, H.A. Offe, Sulfur-containing derivatives of pyridine carboxylic acids and compounds derived therefrom, Chem. Berichte 87 (1954) 825–834.
[32] G. Mazzone, F. Bonina, R. Arrigo-Reina, Synthesis and pharmacological activities of some 2-(alkylaminoalkyl)mercapto-5-aryl-(1,3,4-oxadiazoles), Farmaco, Ed. Scient 32 (1977) 414–429.
[33] R.A. Tromp, S. van Ameijde, C. Pütz, C. Sundermann, B. Sundermann, J.K. von Frijtag Drabbe Künzel, P. IJzerman, Inhibition of nucleoside transport by new analogues of 4-nitrobenzylthioinosine: replacement of the ribose moiety by substituted benzyl groups, J. Med. Chem. 47 (2004) 5441–5450.
[34] S. Chao, S. Li, X. Hui, P. Xu, L. Dong, Synthesis and antibacterial activities of 2-phenyl-5-[[2'-cyano(1,1'-biphenylyl)-4-]methyl]mercapto-1,3,4-oxadiazole, Xinxiang Yixueyuan Xuebao 23 (2006) 5–6.
[35] S. Giri, H. Singh, L.D.S. Yadav, Studies in oxadiazoles. Synthesis of some 2-mercapto-1,3,4-oxadiazoles and related compounds as potential fungicides, Agr. Biol. Chem. 40 (1976) 17–21.
[36] M.C. da Silva Lourenco, M. de Lima Ferreira, M.V.N. de Souza, M.A. Peralta, T.R.A. Vasconcelos, M. das Gracas Henriques, Synthesis and anti-mycobacterial activity of (E)-N'-(monosubstituted-benzylidene)isonicotinohydrazide derivatives, Eur. J. Med. Chem. 43 (2008) 1344–1347.
[37] I. Ninomiya, O. Yamamoto, Photochemistry of isonicotinohydrazide and its analogs in alcohol, Heterocycles 4 (1976) 475–481.
[38] R.R. Shah, R.D. Mehta, A.R. Parikh, Studies on isoniazid derivatives. Preparation and antimicrobial activity of 2-aryl-3-(pyridylcarbomyl)-5-carboxymethyl-4-thiazolidinones, J. Ind. Chem. Soc. 62 (1985) 255–257.
[39] S.K. Boovanahalli, X. Jin, Y. Jin, J.H. Kim, N.T. Dat, Y. Hong, J.H. Lee, S. Jung, K. Lee, J.J. Lee, Synthesis of (aryloxyacetylamino)-isonicotinic/nicotinic acid

analogues as potent hypoxia-inducible factor (HIF)-1a inhibitors, Bioorg. Med. Chem. Lett. 17 (2007) 6305–6310.
[40] M.A. Chowdhury, K.R.A. Abdellatif, Y. Dong, M. Rahman, D. Das, M.R. Suresh, E.E. Knaus, Synthesis of 1-(methanesulfonyl- and aminosulfonylphenyl)acetylenes that possess a 2-(N-difluoromethyl-1,2-dihydropyridin-2-one pharmacophore): evaluation as dual inhibitors of cyclooxygenases and 5-lipoxygenase with anti-inflammatory activity, Bioorg. Med. Chem. Lett. 19 (2009) 584–588.
[41] Q. Zheng, F. Zhang, K. Cheng, Y. Yang, Y. Chen, Y. Qian, H. Zhang, L. Li, C. Zhou, S. An, Q. Jiao, H. Zhu, Synthesis, biological evaluation and molecular docking studies of amide-coupled benzoic nitrogen mustard derivatives as potential antitumor agents, Bioorg. Med. Chem. 18 (2010) 880–886.
[42] A. Molinos-Gómez, X. Vidal, M. Maymó, D. Velasco, J. Martorell, F. López-Calahorra, Tautomeric enhancement of the hyperpolarizability in new acridine-benzothiazolylamine based NLO chromophores, Tetrahedron 61 (2005) 9075–9081.
[43] K. Yamazaki, Y. Kaneko, K. Suwa, S. Ebara, K. Nakazawa, K. Yasuno, Synthesis of potent and selective inhibitors of Candida albicans N-myristoyltransferase based on the benzothiazole structure, Bioorg. Med. Chem. 13 (2005) 2509–2522.
[44] P. Basabe, A. Diego, S. Delgado, D. Díez, I.S. Marcos, J.G. Urones, Short and efficient synthesis of (+)-subersic acids, Tetrahedron 59 (2003) 9173–9177.
[45] M. Ebisawa, M. Ueno, Y. Oshimo, Y. Kondo, Synthesis of dictyomedins using phosphazene base catalyzed diaryl ether formation, Tetrahedron Lett. 48 (2007) 8918–8921.
[46] L. Campeau, M. Parisien, A. Jean, K. Fagnou, Catalytic direct arylation with aryl chlorides, bromides, and iodides: intramoleculas studiel leading tn new intermolecular reactions, J. Am. Chem. Soc. 128 (2006) 581–590.
[47] H.V. Namboodiri, M. Bukhtiyarova, J. Ramcharan, M. Karpusas, Y. Lee, E.B. Springman, Analysis of Imatinib and Sorafenib binding to p38a compared with c-Abl and b-Raf provides structural insights for understanding the selectivity of inhibitors targeting the DFG-Out form of protein kinases, Biochemistry 49 (2010) 3611–3618.
[48] J.R. Simard, M. Getlik, C. Grütter, V. Pawar, S. Wulfert, M. Rabiller, D. Rauh, Development of a fluorescent-tagged kinase assay system for the detection and characterization of allosteric kinase inhibitors, J. Am. Chem. Soc. 131 (2009) 13286–13296.
[49] D. Paquet, R. Bhat, A. Sydow, E. Mandelkow, S. Berg, S. Hellberg, J. Fälting, M. Distel, R.W. Köster, B. Schmid, C. Haass, A zebrafish model of tauopathy allows in vivo imaging of neuronal cell death and drug evaluation, J. Clin. Invest. 119 (2009) 1382–1395.
[50] G.E. Atilla-Gokcumen, D.S. Williams, H. Bregman, N. Pagano, E. Meggers, Organometallic compounds with biological activity: a very selective and highly potent cellular inhibitor for glycogen synthase kinase 3, ChemBioChem 7 (2006) 1443–1450.
[51] C.J. Phiel, C.A. Wilson, V.M.Y. Lee, P.S. Klein, GSK-3 alpha regulates production of Alzheimer's disease amyloid-beta peptides, Nature 423 (2003) 435–439.
[52] M. Cristina da Silva Lourenco, M. de Lima Ferreira, M. Vinícius Nora de Souza, M. Amado Peralta, T. Rocha Alves Vasconcelos, M.O. das Gracas, M. Henriques, Synthesis and anti-mycobacterial activity of (E)-N′-(monosubstituted-benzylidene)isonicotinohydrazide derivatives, Eur. J. Med. Chem. 43 (2008) 1344–1347.
[53] Z. Liberman, H. Eldar-Finkelman, Serine 332 phosphorylation of insulin receptor substrate-1 by glycogen synthase kinase-3 attenuates insulin signaling, J. Biol. Chem. 280 (2005) 4422–4428.
[54] C.B. Kimmel, W.W. Ballard, S.R. Kimmel, B. Ullmann, T.F. Schilling, Stages of embryonic development of the zebrafish, develop, Dynamics 203 (1995) 253–310.